ZU-TH 41/94
IPNO/TH 94-93
STP-DIAS-95-23

Final State Interactions and Khuri-Treiman Equations in $\eta \to 3\pi$ decays [1]

J. Kambor[a], C. Wiesendanger [b,c], D. Wyler[b]

[a] Division de Physique Théorique [2], Institut de Physique Nucléaire, F-91406 Orsay Cedex, France
[b] Theoretische Physik, Universität Zürich, CH-8057 Zürich, Switzerland
[c] Dublin Institute for Advanced Studies, School of Theoretical Physics, 10 Burlington Road, Dublin 4, Ireland

Abstract

Using extended Khuri-Treiman equations, we evaluate the final state interactions due to two-pion rescatterings to the decays $\eta \to \pi^0\pi^+\pi^-$ and $\eta \to \pi^0\pi^0\pi^0$. As subtraction to the dispersion relation we take the one-loop chiral perturbation theory result of Gasser and Leutwyler. The calculated corrections are moderate and amount to about 14% in the amplitude at the center of the decay region. A careful analysis of the errors inherent to our approach is given. As a consequence, the experimental rate of the decay can only be reproduced if the double quark mass ratio $Q^{-2} \equiv \frac{m_d - m_u}{m_s - \hat{m}} \cdot \frac{m_d + m_u}{m_s + \hat{m}}$ is increased from the usual value of $1/(24.1)^2$ to $1/(22.4 \pm 0.9)^2$. We have also calculated the ratio of the rates of the two decays and various Dalitz Plot parameters. In particular, the linear slope a in the charged decay is different from the one-loop value and agrees better with experiment.

[1] Work supported in part by Schweizerischer Nationalfonds.
[2] Unité de Recherche des Universités Paris 11 et Paris 6, associée au CNRS.

1 Introduction

Chiral perturbation theory (ChPT) [1, 2] offers a consistent description of low energy QCD, in particular of the strong and weak mesonic interactions. Whereas most phenomena are quite well accounted for, the predictions for the decays $\eta \to 3\pi$ remain much below the experimental results. The lowest order amplitude is fully determined by chiral symmetry [3] to be

$$\begin{aligned} F(s_a, s_b, s_c) &= -\frac{B_0(m_d - m_u)}{3\sqrt{3}F_0^2} \cdot f^{(2)}(s_a) \\ f^{(2)}(s_a) &\equiv T(s_a) = 1 + \frac{3(s_a - s_0)}{m_\eta^2 - m_\pi^2} \end{aligned} \tag{1.1}$$

where m_u and m_d are the up and down quark masses, F_0 and B_0 QCD parameters and s_a, s_b, s_c, s_0 kinematical variables to be defined later. While the form of eq. (1.1) is valid for the decay into $\pi^0\pi^+\pi^-$, the expression for three neutral pions is obtained by setting $f^{(2)}(s_a) = 1$. Furthermore, in lowest order in the chiral expansion one has

$$\begin{aligned} B_0(m_d - m_u) &= (m_{K^0}^2 - m_{K^+}^2) - (m_{\pi^0}^2 - m_{\pi^+}^2) \\ &\equiv m_1^2. \end{aligned} \tag{1.2}$$

These equations yield a width of 66 eV for the decay $\eta \to \pi^0\pi^+\pi^-$ which is far below the experimental value of 281 ± 28 eV [4]. It is an unusual situation, since most predictions of current algebra fall within 20 to 30% of the experimental results.

However, also the next-to-leading calculation of Gasser and Leutwyler [5] failed to reproduce the experimental value, despite a dramatic improvement. These authors obtain a width of 167 ± 50eV for the $\eta \to \pi^0\pi^+\pi^-$ decay (We have adopted the 'new' value of f_π [6] which increases the width by about 7 eV). Thus, one may conclude that higher order corrections are very large, possibly preventing a satisfactory representation of this decay by ChPT.

Since the decay rate is proportional to $(m_u - m_d)^2$ it is particularly sensitive to the value of the quark masses. The quark mass ratios are known with some precision [7] from a variety of low energy investigations. Since they are fundamental parameters of the basic theory, they should be determined as accurately as possible. Of special interest is the up quark mass because $m_u = 0$ is a very appealing solution to the strong CP problem [8] . From eq. (1.1) we see that decreasing m_u indeed increases the rate as required by experiment. On the other hand, corrections to the second factor will also have this effect. Thus, only a careful investigation of higher order effects will enable one to draw a conclusion on the quark masses.

Let us formulate this more precisely. The amplitude for the decay $\eta \to \pi^0\pi^+\pi^-$ can be written as [5]

$$F(s_a, s_b, s_c) = -\frac{B_0(m_d - m_u)}{3\sqrt{3}F_0^2} \cdot f(s_a, s_b, s_c, \Lambda, m_u, ..) + \text{e.m.} \tag{1.3}$$

where the quark masses are the renormalization group invariant masses, Λ a QCD scale, s_a, s_b, s_c the Mandelstam variables for the decay. Sutherland's theorem [9] implies that the electromagnetic contribution is of order p^2, where p^2 stands for any invariant product of momenta. Moreover, the leading (in momentum) electromagnetic contribution of order $\frac{e^2p^2}{\Lambda^2}$ is further suppressed by a factor $\frac{m_\pi^2}{m_K^2}$ if the amplitude is assumed to be linear in s_a [10, 11]. Recently, these terms were reanalyzed in an effective Lagrangian framework [12] and the expected smallness of the electromagnetic corrections (Sutherland's theorem) was confirmed. We will therefore neglect them throughout.

Returning then to the QCD contribution in eq. (1.3), the second factor, the function f, is expanded in chiral perturbation theory in powers of momentum and mass

$$f = f^{(2)} + f^{(4)} + .. \tag{1.4}$$

Here, $f^{(2)}$ has already been defined in eq. (1.1) and $f^{(4)}$, etc. are of higher orders. $f^{(4)}$ was given explicitely by Gasser and Leutwyler [5] and consists of a variety of loops and counterterms. The corresponding coupling constants also occur in other observables which are also calculated using the chiral Lagrangian, for instance the decay constants or the masses of the mesons. To order p^4, it is therefore possible to express some of these corrections through physical quantities. In particular, the quark mass contribution to the kaon mass difference can be written as [13]

$$\Delta K_{QCD} \equiv (m_{K^0}^2 - m_{K^+}^2)_{QCD} = Q^{-2}\frac{m_K^2}{m_\pi^2}(m_K^2 - m_\pi^2) \tag{1.5}$$

and can be obtained from the measured masses once the electromagnetic mass differences are subtracted. Here,

$$Q^{-2} \equiv \frac{m_d - m_u}{m_s - \hat{m}} \cdot \frac{m_d + m_u}{m_s + \hat{m}} \tag{1.6}$$

with $\hat{m} \equiv \frac{1}{2}(m_d + m_u)$.

Then, one can rewrite the amplitude as

$$\begin{aligned} F(s_a, s_b, s_c) &= -Q^{-2}\frac{m_K^2}{m_\pi^2}(m_K^2 - m_\pi^2)\frac{1}{3\sqrt{3}F_\pi^2} \\ &\quad \cdot f^{(2)}(s_a)(1 + \delta_{DEC}). \end{aligned} \tag{1.7}$$

δ_{DEC} contains the remaining part of the $O(p^4)$ terms as well as corrections from higher orders in the chiral expansion. Terms of order $(m_d - m_u)^2$ are tiny and are therefore neglected throughout. As anticipated, the rate is indeed proportional to the quark mass difference squared. [3]

[3] In passing, we note that in the generalized framework of chiral perturbation theory [14], matters are more complicated and a careful reanalysis of all relations entering eq. (1.7) is required.

The decay $\eta \to 3\pi$ fixes the quantity Q^2 rather than the ratio $\frac{m_u}{m_d}$. This is in agreement with the observation by Kaplan and Manohar [15] that the chiral Lagrangian possesses a curious reparametrization invariance under which masses and some of the other parameters are changed. It implies that matrix elements derived from Green functions which do not involve scalar or pseudoscalar densities are invariant [16] with respect to that transformation. And indeed, the combination Q^2 in eq. (1.6) is invariant, while for instance $\frac{m_u}{m_d}$ is not. Unfortunately, there is no direct experimental access to this ratio, the relevant Green functions must be obtained from semiphenomenological analyses [7].

There exists an independent determination of Q^2 by means of the following equation

$$m_1^2 = \Delta K_{QCD} + (\Delta K - \Delta\pi)_{em}. \tag{1.8}$$

Provided that the electromagnetic contribution is known, eqs. (1.5) and (1.8) can be used to check the consistency of the different calculations or to predict the rate for the decay $\eta \to 3\pi$.

The calculation of the electromagnetic mass differences is notoriously difficult. Dashen's theorem [17] implies that the electromagnetic mass difference of the kaons is equal to the mass difference of the pions, [4] up to terms of order e^2p^2. If these are neglected, one has $\Delta K_{QCD} = m_1^2$ and one can write

$$F(s_a, s_b, s_c) = -\frac{m_1^2}{3\sqrt{3}F_\pi^2} \cdot f^{(2)}(s_a)(1 + \delta_{DEC}) \tag{1.9}$$

and δ_{DEC} determines the rate. In their calculation of the decay rate for $\eta \to 3\pi$ Gasser and Leutwyler [5] obtained a correction δ_{DEC} of about 50%. Together with eq. (1.9), the value of 167 eV for the width results, still far below the experimental number.

However, it was found recently [18, 19] that the corrections to Dashen's theorem could be substantial. One should therefore start from eq. (1.7), avoiding unnecessary uncertainties arising from corrections to Dashen's theorem. The normalization of the $\eta \to 3\pi$ amplitude is then determined by Q^2 which follows in principle from eq. (1.5). As pointed out in [20], the positive corrections to Dashen's theorem found in [18] increase ΔK such that together with the value of δ_{DEC} obtained by Gasser and Leutwyler the experimental rate for $\eta \to 3\pi$ would be reproduced.

Thus, the rate of the η decay can be increased either by determining further corrections in δ_{DEC} (beyond those calculated by Gasser and Leutwyler) or by increasing the value of ΔK_{QCD}. In view of eq. (1.6) this latter term amounts to an increase in Q^2 and thus to a smaller up quark mass. But before any conclusion on the quark masses can be drawn, the decay corrections must be understood better.

It has been argued [21] that $\eta\eta'$ mixing may increase the theoretical rate to the experimental value. However, it was recently shown [22] that the effects of the η' are in fact included in the standard treatment and that the enhancement is due to

[4] the QCD contribution to the pion mass difference is proportional to $(m_d - m_u)^2$ and negligible

an incomplete treatment of the resonances as an explanation for the constants of the chiral Lagrangian. We therefore omit this issue in the following.

The goal of this paper is to calculate one class of corrections in δ_{DEC}, the so called unitary corrections which ensure that the decay amplitude satisfies unitarity. These corrections are the sum of certain diagrams, namely those describing the rescattering of the final state particles to all orders. It is believed that they dominate the corrections, in particular since the final state interactions of two pions in the $I = 0$ s-wave channel is strong and attractive. In fact, in the one-loop calculation of Gasser and Leutwyler they yield the largest new contributions. They account for roughly three quarters of the corrections, pion loops contributing about 85% and kaons and etas about 15% thereof, while other terms provide the remaining quarter (of course, the division of the corrections depends on the renormalization scale chosen; however, physical arguments such as resonance saturation of the counterterms indicate that the scale used for the above numbers is reasonable).

A method to evaluate the unitary corrections has been given long ago by Khuri and Treiman [24]. Keeping only two particle rescatterings of pions (and neglecting p-waves) they derived a set of dispersion relations, the Khuri-Treiman equation. This paper was subsequently analyzed by several authors [25, 26, 27, 28, 29, 30]. In particular, Kacser [28] derived the correct prescription for the analytical continuation of the partial wave projections of the decay amplitude. Bronzan [29] and later also Neveu and Scherk [31] omitting also the $I = 2$ rescatterings, solved the Khuri-Treiman equation approximately. Using the properties of the Omnès function $D(s)$ entering their approximate solution they argued that the remaining terms are small.

Some time ago, Roiesnel and Truong [32] reconsidered the problem, using similar, although not equivalent methods to those of Neveu and Scherk to calculate the unitary corrections. These authors found a large enhancement of the amplitude, enough to account for the observed rate. The numerical results of this work were criticized in Ref. [5] on physical grounds and we confirm their findings. We believe therefore that their result is a overestimate of the unitary corrections.

In this work we will use (and generalize by the inclusion of p-waves (see also [33])) the method of Khuri and Treiman to determine numerically the unitary corrections. It is organized as follows.

In section 2, after rewieving the decay amplitude for $\eta \to 3\pi$ and giving the necessary definitions, we formulate the Khuri-Treiman equations and the inclusion of the $I = 1$ rescatterings. In section 3 we discuss the subtraction procedure, and in section 4 we build up an iterative scheme for the numerical solution of the set of coupled equations for the projected amplitudes U, V, W. In section 5 we discuss our numerical results and the quality of our iteration and in section 6 we draw the conclusions. Some appendices contain necessary technical details.

2 The dispersion relations

2.1 Isospin decomposition for the amplitude

We begin with a short review of the amplitude for the decay $\eta \to 3\pi$. It serves to fix the notation, give the isospin decomposition and to discuss its symmetry properties.

We denote the three pions in the decay $\eta \to 3\pi$ by the letters a,b,c, their corresponding four-momenta by k_a, k_b, k_c and label their isospins by α, β, γ. The invariant masses of the pions are then $k_a^2 = k_b^2 = k_c^2 = m_\pi^2$ disregarding all mass differences at this stage. The four momentum of the isospin singlet η is denoted by k_r.

In the standard model of the strong, electromagnetic and weak interactions, the decay $\eta \to 3\pi$ proceeds either through the isospin breaking piece of the QCD hamiltonian or through an operator of electromagnetic origin. For both contributions, the interaction Hamiltonian $H(0)$ is $\Delta I = 1$. It is then convenient to treat the η as a spurious isospin triplet and to assume isospin conservation in the decay. The corresponding isospin state is labeled by ρ.

The amplitude for a general isospin assignment of the pions is

$$\begin{aligned} M &= <\alpha, k_a; \beta, k_b; \gamma, k_c|H(0)|k_r> \\ &\equiv i(2\pi)^4\delta(k_a + k_b + k_c - k_r)M_{\alpha\beta\gamma;\rho}(s_a, s_b, s_c). \end{aligned} \tag{2.1}$$

The invariant amplitude has the decomposition

$$\begin{aligned} M_{\alpha\beta\gamma;\rho}(s_a, s_b, s_c) &= F(s_a, s_b, s_c)\delta_{\beta\gamma}\delta_{\alpha\rho} \\ &\quad +F(s_b, s_c, s_a)\delta_{\alpha\gamma}\delta_{\beta\rho} \\ &\quad +F(s_c, s_a, s_b)\delta_{\alpha\beta}\delta_{\gamma\rho}, \end{aligned} \tag{2.2}$$

where the isoscalar amplitude F is a function of the Mandelstam variables

$$s_a = (k_r - k_a)^2, \quad s_b = (k_r - k_b)^2, \quad s_c = (k_r - k_c)^2, \tag{2.3}$$

which are related by the on-shell condition

$$s_a + s_b + s_c = 3m_\pi^2 + m_\eta^2 \equiv 3s_0. \tag{2.4}$$

Bose statistics of the three pion system implies the symmetry

$$F(s_a, s_b, s_c) = F(s_a, s_c, s_b) \tag{2.5}$$

such that the amplitude $M_{\alpha\beta\gamma;\rho}(s_a, s_b, s_c)$ remains invariant under the exchanges of

$$\begin{aligned} a &\rightleftharpoons a \qquad b \rightleftharpoons c, \\ b &\rightleftharpoons b \qquad c \rightleftharpoons a, \\ c &\rightleftharpoons c \qquad a \rightleftharpoons b. \end{aligned} \tag{2.6}$$

The amplitude for the decay into charged pions is then found to be

$$< \pi^+, \pi^-, \pi^0 | H(0) | \eta >= i(2\pi)^4 \delta(k_a + k_b + k_c - k_r) F(s_a, s_b, s_c), \tag{2.7}$$

whereas the amplitude for the decay into neutral pions is expressed as

$$\begin{aligned} < \pi^0, \pi^0, \pi^0 | H(0) | \eta > \; &= \; i(2\pi)^4 \delta(k_a + k_b + k_c - k_r) \\ &\quad [F(s_a, s_b, s_c) + F(s_b, s_c, s_a) + F(s_c, s_a, s_b)] \, . \end{aligned} \tag{2.8}$$

2.2 Isospin sum and scalar dispersion relation

We begin with the dispersion representation for the decay amplitude eq. (2.2) derived by Khuri and Treiman [24]

$$\begin{aligned} M_{\alpha\beta\gamma;\rho}(s_a, s_b, s_c) \; &= \; \frac{1}{\pi} \int_4^\infty ds'_a \frac{\text{disc}_{|a} M_{\alpha\beta\gamma;\rho}(s'_a, s_b, s_c)}{s'_a - s_a - i\varepsilon} \\ &+ \; \frac{1}{\pi} \int_4^\infty ds'_b \frac{\text{disc}_{|b} M_{\beta\gamma\alpha;\rho}(s_a, s'_b, s_c)}{s'_b - s_b - i\varepsilon} \\ &+ \; \frac{1}{\pi} \int_4^\infty ds'_c \frac{\text{disc}_{|c} M_{\gamma\alpha\beta;\rho}(s_a, s_b, s'_c)}{s'_c - s_c - i\varepsilon} . \end{aligned} \tag{2.9}$$

Here and below, all momenta and masses are taken in units of m_π; in particular, the mass of the η will be denoted by m.

Eqn.(2.9) expresses the connection between causality and analyticity for the considered amplitude. Unitarity gives an expression for the discontinuity of $M_{\alpha\beta\gamma;\rho}$ in s_a for fixed s_c and analogous ones for the other two discontinuities in the form of a sum over intermediate states involved in all the rescattering processes. The intermediate state with lowest mass contributing in this sum is the two-pion state leading to a rescattering of two outgoing pions in the decay. As any other intermediate state such as a $\bar{K}K$ or a 4π state will contribute to the discontinuity at a much larger threshold it is a reasonable approximation to drop them [24]. Hence, we find

$$\begin{aligned} 2i \, \text{disc}_{|a} M_{\alpha\beta\gamma;\rho}(s_a, s_b, s_c) = \frac{i}{2!} \sum_{\delta,\varepsilon} \int d\tilde{p}_d d\tilde{p}_e \\ (2\pi)^4 \delta(k_r - k_a - p_d - p_e) N^*_{\delta\varepsilon;\beta\gamma}(s_a, s'_d, s'_e) \cdot M_{\alpha\delta\varepsilon;\rho}(s_a, s_d, s_e) \end{aligned} \tag{2.10}$$

where p_d and p_e are the four-momenta of the intermediate pions d, e. In eq. (2.10) we have introduced the invariant pion-pion scattering matrix element

$$\begin{aligned} &< \alpha, k_a; \beta, k_b | T | \varepsilon, p_e; \eta, p_f > \\ &\quad \equiv i(2\pi)^4 \delta(k_a + k_b - p_e - p_f) N_{\alpha\beta;\varepsilon\eta}(s_a, s'_d, s'_e) \end{aligned} \tag{2.11}$$

and the phase space measure for the intermediate pions

$$d\tilde{p} \equiv \frac{d^3 p}{(2\pi)^3 2E}, \qquad E = \sqrt{p^2 + 1}. \tag{2.12}$$

The variables s'_d and s'_e are defined by

$$\begin{aligned} s'_d &= (k_b - p_d)^2 \\ s'_e &= (k_b - p_e)^2 \end{aligned} \tag{2.13}$$

In the Khuri-Treiman approximation, the discontinuity of the decay amplitude becomes thus just a product of the pion scattering amplitude with the decay amplitude itself.

To perform the phase space integrals in eq. (2.10), one usually chooses the c. m. frame of the rescattered pions defined by $\underline{k}_b + \underline{k}_c = 0$. Letting the θ-angle in $d\tilde{p}_d$ to be the angle θ_{da} between $\underline{k}_a$ and $\underline{p}_d$ the discontinuity becomes

$$\begin{aligned} &\text{disc}_{|a} M_{\alpha\beta\gamma;\rho} = \frac{1}{32\pi}\beta(s_a) \\ &\sum_{\delta,\varepsilon} \int \frac{d\Omega_{da}}{4\pi} N^*_{\delta\varepsilon;\beta\gamma}(s_a, \cos\theta_{bd}) \cdot M_{\alpha\delta\varepsilon;\rho}(s_a, \cos\theta_{da}) \end{aligned} \tag{2.14}$$

where we have introduced the shorthand notation

$$\beta(s) \equiv \sqrt{\frac{s-4}{s}}. \tag{2.15}$$

We note that some of the kinematical variables are not well behaved in the decay region; we shall supplement a correct analytic interpretation for them below.

Adopting the normalizations from Ref. [34], we continue with the isospin decomposition of the invariant pion-pion scattering matrix element

$$\begin{aligned} N_{\alpha\beta;\gamma\delta}(s_a, s_b, s_c) &= \frac{1}{3}(T^0(s_a, s_b, s_c) - T^2(s_a, s_b, s_c))\delta_{\alpha\beta}\delta_{\gamma\delta} \\ &+ \frac{1}{2}(T^2(s_a, s_b, s_c) + T^1(s_a, s_b, s_c))\delta_{\alpha\gamma}\delta_{\beta\delta} \\ &+ \frac{1}{2}(T^2(s_a, s_b, s_c) - T^1(s_a, s_b, s_c))\delta_{\alpha\delta}\delta_{\beta\gamma} \end{aligned} \tag{2.16}$$

where the T^I are the isospin amplitudes to isospin I. In our frame of reference they depend on two variables only, the total invariant mass of the pions and the intermediate scattering angle θ_{bd}. The corresponding isospin decomposition of the decay amplitude has already been given in eq. (2.2).

We now insert eq. (2.16) into eq. (2.14) and use eq. (2.2). This yields, for the discontinuity of M in s_a

$$\begin{aligned} &\text{disc}_{|a} M^1_{\alpha\beta\gamma;\rho} = \frac{1}{32\pi}\beta(s_a) \int \frac{d\Omega_{da}}{4\pi} \\ &[\delta_{\beta\gamma}\delta_{\alpha\rho}\{T^{0*}(s_a, s'_d, s'_e)F(s_a, s_d, s_e) \\ &+\frac{1}{3}(T^{0*}(s_a, s'_d, s'_e) - T^{2*}(s_a, s'_d, s'_e))F(s_e, s_a, s_d) \end{aligned}$$

$$+\frac{1}{3}(T^{0*}(s_a,s'_d,s'_e)-T^{2*}(s_a,s'_d,s'_e))F(s_d,s_e,s_a)\}$$
$$+\delta_{\gamma\alpha}\delta_{\beta\rho}\{\frac{1}{2}(T^{2*}(s_a,s'_d,s'_e)+T^{1*}(s_a,s'_d,s'_e))F(s_d,s_e,s_a)$$
$$+\frac{1}{2}(T^{2*}(s_a,s'_d,s'_e)-T^{1*}(s_a,s'_d,s'_e))F(s_e,s_a,s_d)\}$$
$$+\delta_{\alpha\beta}\delta_{\gamma\rho}\{\frac{1}{2}(T^{2*}(s_a,s'_d,s'_e)+T^{1*}(s_a,s'_d,s'_e))F(s_e,s_a,s_d)$$
$$+\frac{1}{2}(T^{2*}(s_a,s'_d,s'_e)-T^{1*}(s_a,s'_d,s'_e))F(s_d,s_e,s_a)\}]. \tag{2.17}$$

Next, we use this result and the two analogous ones for the discontinuities in s_b and s_c in the dispersion representation eq. (2.9) for the full amplitude. Comparing the coefficients in the different isospin channels we obtain three dispersion relations for the scalar functions F [24]:

$$\begin{aligned}
F(s_a,s_b,s_c) &= \frac{1}{\pi}\int_4^\infty \frac{ds'_a}{s'_a-s_a-i\varepsilon}\frac{1}{32\pi}\beta(s'_a)\int\frac{d\Omega_{da}}{4\pi} \\
&\quad \{T^{0*}(s'_a,s'_d,s'_e)F(s'_a,s_d,s_e) \\
&\quad +\frac{1}{3}(T^{0*}(s'_a,s'_d,s'_e)-T^{2*}(s'_a,s'_d,s'_e))F(s_d,s_e,s'_a) \\
&\quad +\frac{1}{3}(T^{0*}(s'_a,s'_d,s'_e)-T^{2*}(s'_a,s'_d,s'_e))F(s_e,s'_a,s_d)\} \\
&+ \frac{1}{\pi}\int_4^\infty \frac{ds'_b}{s'_b-s_b-i\varepsilon}\frac{1}{32\pi}\beta(s'_b)\int\frac{d\Omega_{db}}{4\pi} \\
&\quad \{\frac{1}{2}(T^{2*}(s'_b,s'_d,s'_e)+T^{1*}(s'_b,s'_d,s'_e))F(s_e,s'_b,s_d) \\
&\quad +\frac{1}{2}(T^{2*}(s'_b,s'_d,s'_e)-T^{1*}(s'_b,s'_d,s'_e))F(s_d,s_e,s'_b)\} \\
&+ \frac{1}{\pi}\int_4^\infty \frac{ds'_c}{s'_c-s_c-i\varepsilon}\frac{1}{32\pi}\beta(s'_c)\int\frac{d\Omega_{dc}}{4\pi} \\
&\quad \{\frac{1}{2}(T^{2*}(s'_d,s'_e,s'_c)+T^{1*}(s'_c,s'_d,s'_e))F(s_d,s_e,s'_c) \\
&\quad +\frac{1}{2}(T^{2*}(s'_c,s'_d,s'_e)-T^{1*}(s'_c,s'_d,s'_e))F(s_e,s'_c,s_d)\}.
\end{aligned} \tag{2.18}$$

The invariant variables s_d, s_e, s'_d, s'_e must be expressed in terms of s_a, s_b, s_c. The other two scalar dispersion representations are obtained from eq. (2.18) by permutation of a, b, c.

To evaluate further this dispersion relation we retain only the s- and p-wave contributions to the rescattering. The relevant partial wave expansions of the pion scattering amplitudes T^I for fixed isospin I are given as usual by [34]

$$T^I(s,\cos\theta)=\frac{32\pi}{\beta(s)}\sum_0^\infty(2l+1)P_l(\cos\theta)f_l^I(s) \tag{2.19}$$

where s is the total invariant mass and θ the scattering angle in the c.m. system of the colliding pions. In the elastic region $4 < s < 16$, the partial wave amplitudes are parametrized by real phase shifts as

$$f_l^I(s) = e^{i\delta_l^I(s)} \sin \delta_l^I(s). \tag{2.20}$$

The lowest contributions for $I = 0, 2$ are s-waves

$$\begin{aligned} T^0(s) &= \frac{32\pi}{\beta(s)} f_0^0(s) \\ T^2(s) &= \frac{32\pi}{\beta(s)} f_0^2(s) \end{aligned} \tag{2.21}$$

while for $I = 1$ it is a p-wave

$$T^1(s, \cos\theta) = \frac{32\pi}{\beta(s)} 3 \cos\theta \cdot f_1^1(s). \tag{2.22}$$

The factors $\frac{1}{32\pi}\beta$ in (2.18) just cancel now against the corresponding factors in the partial wave expansion of T^I and we are left with two types of angle integrals.

In the case of s-wave contributions the pion-pion rescattering is isotropic. For $I = 0, 2$ we have thus angle integrations of the type [24]

$$\begin{aligned} \overline{F}(s_a) &\equiv \int \frac{d\Omega_{da}}{4\pi} F(s_a, s_d, s_e) \\ \tilde{F}(s_a) &\equiv \int \frac{d\Omega_{da}}{4\pi} F(s_d, s_e, s_a) \end{aligned} \tag{2.23}$$

where s_d, s_e are expressed through s_a and $\cos\theta_{da}$ as

$$\begin{aligned} s_e &= 3s_0 - s_a - s_d \\ s_d &= \frac{3s_0 - s_a}{2} + K(s_a) \cdot \cos\theta_{da} \\ d\Omega_{da} &= d\varphi \cdot d\cos\theta_{da}. \end{aligned} \tag{2.24}$$

Here we introduced the Kacser function [28]

$$K(s) \equiv \sqrt{\frac{(s-4)(s-(m-1)^2)(s-(m+1)^2)}{4s}}. \tag{2.25}$$

Its cuts and limits in the complex s-plane will be discussed below.

We may now recast the integrations above as integrations over s_d and obtain

$$\overline{F}(s_a) = \frac{1}{2K(s_a)} \int_{s_{d-}(s_a)}^{s_{d+}(s_a)} ds_d \, F(s_a, s_d, 3s_0 - s_a - s_d) \tag{2.26}$$

and in an analogous way

$$\tilde{F}(s_a) = \frac{1}{2K(s_a)} \int_{s_{d-}(s_a)}^{s_{d+}(s_a)} ds_d \, F(s_d, 3s_0 - s_a - s_d, s_a) \tag{2.27}$$

where

$$s_{d+}(s) \equiv \frac{3s_0 - s}{2} + K(s), \quad s_{d-}(s) \equiv \frac{3s_0 - s}{2} - K(s). \tag{2.28}$$

The integral $\tilde{F}(s_a)$ obeys the symmetry property

$$\tilde{F}(s_a) = \frac{1}{2K(s_a)} \int_{s_{d-}(s_a)}^{s_{d+}(s_a)} ds_d F(3s_0 - s_a - s_d, s_a, s_d) \tag{2.29}$$

which follows immediately from the Bose symmetry properties of F itself and a change of variable $s_d \to 3s_0 - s_a - s_d$.

The p-wave contribution for $I = 1$ leads to the more complicated integral

$$I(s_a, s_b, s_c) \equiv \int \frac{d\Omega_{da}}{4\pi} \cos\theta_{bd} F(s_e, s_a, s_d). \tag{2.30}$$

In order to perform the angle integration explicitly and to get rid of the two angles we invoke a partial wave expansion for F

$$F(s_e, s_a, s_d) = \sum_0^\infty (2l+1) P_l(\cos\theta_{da}) F_l^{s_d}(s_a). \tag{2.31}$$

Making use of well-known properties of the Legendre polynomials we obtain

$$I(s_a, s_b, s_c) = \cos\theta_{ba} \cdot F_1^{s_d}(s_a). \tag{2.32}$$

The $l = 1$ projection of F is next expressed as an integral over s_d

$$\begin{aligned} F_1^{s_d}(s_a) &= \frac{1}{4K^2(s_a)} \int_{s_{d-}(s_a)}^{s_{d+}(s_a)} ds_d \, (2s_d + s_a - 3s_0) \\ &\quad \cdot F(3s_0 - s_a - s_d, s_a, s_d) \end{aligned} \tag{2.33}$$

and $\cos\theta_{ba}$ is recast as

$$\cos\theta_{ba} = \frac{s_b - s_c}{2K(s_a)}. \tag{2.34}$$

Plugging all together we obtain the desired expression

$$I(s_a, s_b, s_c) = \frac{s_b - s_c}{3} \hat{F}(s_a), \tag{2.35}$$

defining the function of one variable

$$\begin{aligned} \hat{F}(s_a) &\equiv \frac{3}{8K^3(s_a)} \int_{s_{d-}(s_a)}^{s_{d+}(s_a)} ds_d \, (2s_d + s_a - 3s_0) \\ &\quad \cdot F(3s_0 - s_a - s_d, s_a, s_d). \end{aligned} \tag{2.36}$$

$I(s_a, s_b, s_c)$ satisfies

$$\begin{aligned} I(s_a, s_b, s_c) &= -\frac{s_b - s_c}{8K^3(s_a)} \int_{s_{d-}(s_a)}^{s_{d+}(s_a)} ds_d \, (2s_d + s_a - 3s_0) \\ &\quad \cdot F(s_d, 3s_0 - s_a - s_d, s_a) \end{aligned} \tag{2.37}$$

following from the Bose symmetry properties of F and a change of variable $s_d \to 3s_0 - s_a - s_d$ This will allow us to rewrite the integral equation for $F(s_a, s_b, s_c)$ as an equivalent set of coupled integral equations for functions of one variable only.

Note that the projections as given in eqs. (2.26), (2.27) and (2.36) are defined only for values of s_a in the physical decay region $4 < s_a < (m-1)^2$. Outside this range, the argument of the square root in the Kacser function eq. (2.25) becomes negative and we have to give this funcion a meaning by appropriate analytic continuation. This was studied by Bronzan and Kacser [27, 28] whom we follow closely. Based on comparison with explicit expressions for the projection operation in perturbation theory and demanding that the general definition of the projection should reduce to these expressions, they find that the naive integrals have to be replaced by contour integrals in the complex s_d-plane. The respective paths joining $s_{d-}(s_a)$ with $s_{d+}(s_a)$ must avoid the real axis for $4 < s_d < \infty$ as the amplitude F has a cut there. Where necessary, $s_{d-}(s_a)$ and $s_{d+}(s_a)$ are taken infinitesimally above or below the real axis according to the prescription obtained by replacing $m^2 \to m^2 + i\delta$, $\delta \to 0+$ for real s_a. Hence, we will consider the projections above, eqs. (2.26) (2.27) (2.36), as contour integrals with suitable integration pathes and introduce the function H

$$H(s) \equiv \sqrt{\frac{|(s-4)(s-(m-1)^2)(s-(m+1)^2)|}{|4s|}} \tag{2.38}$$

which is well defined for all s different from zero and allows us to express the necessaranalytic continuation of the Kacser function K in a simple way.

Next we turn to the description of the different paths in the s_d-plane belonging to the four cases we have to discuss if evaluating the aforementioned definition of the projection operation. We must distinguish four cases.
i) $4 < s_a < \frac{m^2-1}{2}$: as s_a is in the physical decay region $K(s_a)$ coincides with $H(s_a)$. (see Fig. 1a). The end points of the contour are lying infinitesimally above the real axis and are found to be

$$\begin{aligned} s_{d+}(s_a) &= \frac{3s_0 - s_a}{2} + H(s_a) + i\delta, \qquad (2.39) \\ s_{d-}(s_a) &= \frac{3s_0 - s_a}{2} - H(s_a) + i\delta. \end{aligned}$$

ii) $\frac{m^2-1}{2} < s_a < (m-1)^2$: s_a is still in the physical decay region so that $K(s_a)$ coincides with $H(s_a)$ again. The point $s_a = \frac{m^2-1}{2}$ is important because when s_a goes through it, the endpoint $s_{d-}(s_a)$ continuously turns around the beginning of the cut at 4 and remains then infinitesimally below the real axis (see Fig. 1b) such that only the other endpoint $s_{d+}(s_a)$ of the contour remains infinitesimally above the real axis. The two end points are now found to be

$$s_{d+}(s_a) = \frac{3s_0 - s_a}{2} + H(s_a) + i\delta, \tag{2.40}$$

$$s_{d-}(s_a) = \frac{3s_0 - s_a}{2} - H(s_a) - i\delta. \tag{2.41}$$

iii) $(m-1)^2 < s_a < (m+1)^2$: as s_a has left the physical decay region $K(s_a)$ must be analytically continued and is defined to be $K(s_a) \equiv iH(s_a)$. The endpoint $s_{d-}(s_a)$ turns now smoothly into the half plane below the real axis whereas the other endpoint $s_{d+}(s_a)$ turns smoothly into the half plane above the real axis in a symmetric fashion such that

$$s_{d+}(s_a) = \frac{3s_0 - s_a}{2} + iH(s_a), \quad s_{d-}(s_a) = \frac{3s_0 - s_a}{2} - iH(s_a). \tag{2.42}$$

The most adequate contour for numerical purposes joining those two points follows just the path the end points move along if s_a goes from $(m-1)^2$ to $(m+1)^2$ (see Fig. 1c) and is thus parametrized by s itself as shown in eqns.(2.42).
iv) $(m+1)^2 < s_a$: as s_a is out of the physical decay region $K(s_a)$ must again be analytically continued and is defined to be $K(s_a) \equiv -H(s_a)$ (see Fig. 1d). The end points of the contour are lying in this case on the real axis

$$s_{d+}(s_a) = \frac{3s_0 - s_a}{2} - H(s_a), \quad s_{d-}(s_a) = \frac{3s_0 - s_a}{2} + H(s_a). \tag{2.43}$$

Note that at $s_a = (m-1)^2$ the projections of a function with a cut have a singularity because K vanishes at this point whereas the integration contour still has finite length and the integral over the imaginary part of the function along the contour does not vanish. The actual form of this singularity for $\overline{F}(s_a)$ around $s_a = (m-1)^2$ is then given by

$$\overline{F}(s_a) \sim \frac{1}{((m-1)^2 - s_a)^{\frac{1}{2}}} \cdot \text{const.} \tag{2.44}$$

and for $\hat{F}(s_a)$ by

$$\hat{F}(s_a) \sim \frac{1}{((m-1)^2 - s_a)^{\frac{3}{2}}} \cdot \text{const.} \tag{2.45}$$

where the constant is in fact the value of the contour integral for $s_a = (m-1)^2$. We will use this form later to analyse the consequences of this pole in the projection prescription.

The projection operations occuring in the eqs. (2.26), (2.27) and (2.36) are now given by well defined contour integrals and we use them in the further evaluation of the integral equation (2.18) for F. We thus insert the partial wave expansions of T^I in the expression (2.18) for the scalar function F. Using the definitions (2.26), (2.27) and (2.36) for the different projections and including the subtraction polynomial as required by the discussion in section 3, we may recast F in the following way

$$\begin{aligned} F(s_a, s_b, s_c) &= P(s_a, s_b, s_c) + U(s_a) + V(s_b) + V(s_c) \\ &+ (s_c - s_a) \cdot W(s_b) + (s_b - s_a) \cdot W(s_c) \end{aligned} \tag{2.46}$$

where we defined the functions of one variable U, V, W

$$U(s_a) = \frac{\prod_{i=1}^3 (s_a - s_i)}{\pi} \int_4^\infty \frac{ds'_a}{\prod_{j=1}^3 (s'_a - s_j)(s'_a - s_a - i\varepsilon)} \cdot \{f_0^{0*}(s'_a)\overline{F}(s'_a) + \frac{2}{3}(f_0^{0*}(s'_a) - f_0^{2*}(s'_a))\tilde{F}(s'_a)\}, \tag{2.47}$$

$$V(s_a) = \frac{\prod_{i=1}^3 (s_a - s_i)}{\pi} \int_4^\infty \frac{ds'_a}{\prod_{j=1}^3 (s'_a - s_j)(s'_a - s_a - i\varepsilon)} \cdot f_0^{2*}(s'_a)\tilde{F}(s'_a) \tag{2.48}$$

and

$$W(s_a) = \frac{(s_a - s_1)(s_a - s_2)}{3\pi} \int_4^\infty \frac{ds'_a}{(s'_a - s_1)(s'_a - s_2)(s'_a - s_a - i\varepsilon)} \cdot f_1^{1*}(s'_a)\hat{F}(s'_a) + \text{perm.}, \tag{2.49}$$

where perm. denotes the symmetrization of W in s_1, s_2, s_3. Note that, unlike U and V, the function W is subtracted only twice. As ChPT yields the amplitude F only to the accuracy p^4 and as W is multiplied by factors of $O(p^2)$ we can not make three subtractions here. On the other hand, convergence of the integral is still ensured as the p-wave projection brings an extra factor of $\frac{1}{s'_a}$ coming from the Kacser function K in the integrand.

Numerically it is easier to deal with three integral equations for three functions of one variable than with one such equation for a function of three variables. We thus have to transform the content of the subtracted dispersion representation eq. (2.18) for F by taking its s- and p-wave projections. Note that all projections of functions of one variable are either trivial or may be expressed as a "bar-projection" (see eq. (2.26), where each argument s_c is understood to be expressed by the integration variable s_b and constant terms by

$$s_c = 3s_0 - s_a - s_b. \tag{2.50}$$

The projections become now

$$\begin{aligned}
\overline{F}(s_a) &= \overline{P}(s_a) + U(s_a) + \overline{V}_b(s_a) + \overline{V}_c(s_a) \\
&+ \overline{(s_c - s_a)W_b}\,(s_a) + \overline{(s_b - s_a)W_c}\,(s_a), \\
\tilde{F}(s_a) &= \tilde{P}(s_a) + \overline{U}_b(s_a) + \overline{V}_c(s_a) + V(s_a) \\
&+ \overline{(s_a - s_b)W_c}\,(s_a) \\
\hat{F}(s_a) &= \hat{P}(s_a) + \frac{3}{4K^2(s_a)}\{\overline{(s_b - s_c)U_c}\,(s_a) + \overline{(s_b - s_c)V_b}\,(s_a) \\
&+ \overline{(s_b - s_c)^2 \cdot W}(s_a) + \overline{(s_b - s_c)(s_a - s_c)W_b}\,(s_a)\}
\end{aligned}$$

where the subscripts b, c denote the argument of the respective function under the projection integral. Note that certain terms vanish because $\overline{s_b - s_c} = 0$. We next change arguments of the functions above to s_b and omit in the following the subscripts making use of the relations

$$\begin{aligned} \overline{A}_c(s_a) &= \overline{A}_b(s_a) \\ \overline{s_b\, A_c}(s_a) &= \overline{s_c\, A_b}(s_a) \\ \overline{s_c\, A_c}(s_a) &= \overline{s_b\, A_b}(s_a) \end{aligned} \tag{2.51}$$

where A denotes any of the functions U, V, W. Eqs.(2.51) are thus rewritten as

$$\begin{aligned} \overline{F}(s_a) &= \overline{P}(s_a) + U(s_a) + 2\overline{V}(s_a) \\ &+ 2\overline{(s_c - s_a)W}\,(s_a), \\ \tilde{F}(s_a) &= \tilde{P}(s_a) + \overline{U}(s_a) + V(s_a) + \overline{V}(s_a) \\ &+ \overline{(s_a - s_c)W}\,(s_a), \\ \hat{F}(s_a) &= \hat{P}(s_a) + \frac{3}{4K^2(s_a)}\{\overline{(s_c - s_b)U}\,(s_a) + \overline{(s_b - s_c)V}\,(s_a) \\ &+ \overline{(s_b - s_c)^2}\cdot W(s_a) + \overline{(s_b - s_c)(s_a - s_c)W}\,(s_a)\}. \end{aligned}$$

Finally, we insert eqs. (2.52) for the projections expressed in terms of U, V, W into the defining eq. (2.47) for U, eq. (2.48 for V and (2.49) for W. This yields the coupled system

$$\begin{aligned} U(s_a) &= \frac{\prod_{i=1}^3 (s_a - s_i)}{\pi} \int_4^\infty \frac{ds'_a}{\prod_{j=1}^3 (s'_a - s_j)(s'_a - s_a - i\varepsilon)} \\ &\cdot\{f_0^{0*}(s'_a)\,[\overline{P}(s'_a) + \frac{2}{3}\tilde{P}(s'_a) + U(s'_a) + \frac{2}{3}\overline{U}(s'_a) \\ &+ \frac{2}{3}V(s'_a) + \frac{8}{3}\overline{V}(s'_a) + \frac{4}{3}\overline{(s_c - s_a)W}\,(s'_a)] \\ &- f_0^{2*}(s'_a)\,[\frac{2}{3}\tilde{P}(s'_a) + \frac{2}{3}\overline{U}(s'_a) + \frac{2}{3}V(s'_a) \\ &+ \frac{2}{3}\overline{V}(s'_a) + \frac{2}{3}\overline{(s_a - s_c)W}\,(s'_a)]\}, \end{aligned} \tag{2.52}$$

$$\begin{aligned} V(s_a) &= \frac{\prod_{i=1}^3 (s_a - s_i)}{\pi} \int_4^\infty \frac{ds'_a}{\prod_{j=1}^3 (s'_a - s_j)(s'_a - s_a - i\varepsilon)} \\ &\cdot f_0^{2*}(s'_a)\,[\tilde{P}(s'_a) + \overline{U}(s'_a) + V(s'_a) \\ &+ \overline{V}(s'_a) + \overline{(s_a - s_c)W}\,(s'_a)] \end{aligned} \tag{2.53}$$

and

$$W(s_a) = \frac{(s_a - s_1)(s_a - s_2)}{3\pi} \int_4^\infty \frac{ds'_a}{(s'_a - s_1)(s'_a - s_2)(s'_a - s_a - i\varepsilon)}$$

$$\cdot f_1^{1*}(s'_a)\,[\hat{P}(s'_a) + \frac{3}{4K^2(s'_a)}\{\overline{(s_c - s_b)U}\,(s'_a) + \overline{(s_b - s_c)V}\,(s'_a) \quad (2.54)$$
$$+\overline{(s_b - s_c)^2}\cdot W(s'_a) + \overline{(s_b - s_c)(s_a - s_c)W}\,(s'_a)\}]$$
$$+ \quad \text{perm.}$$

These are our final expressions which generalize the Khuri-Treiman equations. As we mentioned above there are in fact singularities in the projected functions occuring under the integrals. The question of whether this leads to problems in the reconstruction of the amplitude by the dispersion integrals will be analysed in section 4.

3 Subtractions

The generalized Khuri-Treiman equations in (2.46-2.49) have been formulated with three subtractions, because we will use them in this form. However, as usual in dispersion relation techniques, the number of subtractions is to a large extent arbitrary. The minimal number of subtractions is determined by the high energy behaviour of the amplitude. If this is known, one is of course still free to take more subtractions than necessary for convergence. With fewer subtractions, the dispersion integral is more weakly convergent and depends more strongly on the poorly known high energy behaviour of the scattering phase. Conversely, if many subtractions are used the integral is better behaved; however then we need a larger number of subtraction constants which in general are less well known. Thus, one must keep a delicate balance in order to optimally use the available data and their uncertainties.

The asymptotic behaviour of the $\eta \to 3\pi$ amplitude may be indicated by Regge phenomenology. Since there is no pomeron exchange in $\eta\pi \to \pi\pi$, the leading Regge trajectory is the one associated with the ρ; we therefore expect an asymptotic behaviour $A \sim s_a^{1/2}$ $(s_b = 0)$ for the $I = 1$ component of the amplitude in the t-channel. The $I = 0, 2$ components are not affected by ρ-exchange and are expected to approach a constant asymptotically. In order to ensure convergence, it is thus sufficient to subtract the dispersion relation once.

However, our calculational scheme of dealing with $\pi\pi$ final state interactions relies on elastic unitarity. In the $I = 0$ s-wave channel the phase shift exhibits large inelasticities above 1 GeV. Therefore it is desirable that this region is unimportant in the evaluation of the dispersion integrals. It turns out that this requirement implies at least two subtractions. We will discuss the influence of the phase shifts above 1 GeV on our results in sect. 5.

Besides the final state interactions we are attempting to control, there are also mass corrections to the $\eta \to 3\pi$ amplitude. These are also known at the one-loop level where the total amplitude is [5]

$$A^{1-\text{loop}}(s_a, s_b, s_c) \quad = \quad -\frac{Q^{-2}\frac{m_K^2}{m_\pi^2}(m_K^2 - m_\pi^2)}{3\sqrt{3}F_\pi^2} \times \bar{A}(s_a, s_b, s_c),$$

$$\bar{A}(s_a,s_b,s_c) \;=\; T(s_a)+\mathcal{U}(s_a,s_b,s_c)+\mathcal{V}(s_a)+\mathcal{W}(s_a,s_b,s_c). \qquad (3.1)$$

The leading order expression $T(s_a)$ is given in eq. (1.1) and the other terms will be discussed below. $\mathcal{U}(s_a,s_b,s_c)$ denotes the unitarity corrections and $\mathcal{V}(s_a)$, $\mathcal{W}(s_a,s_b,s_c)$ are polynomials in s_a,s_b,s_c resulting from tadpole and tree graphs at order p^4 in the low energy expansion. $\mathcal{U}(s_a,s_b,s_c)$ contains the two-pion $I=0,1$ and 2 final state interactions. These rescattering graphs are primarily responsible for a large enhancement of the amplitude at next-to-leading order. However, as discussed in great detail in Ref. [5], only the sum of all terms in eq. (3.1) is a meaningful quantity: the magnitude of the final state interactions of the pions depends on the manner in which the unitarity corrections are split off from the rest.

In this work we use the ChPT one-loop amplitude to obtain an improved estimate for the subtraction polynomial entering the generalized Khuri-Treiman equations. There are three important points here: i) As mentioned above the one-loop amplitude contains already some final state interactions. In order to avoid double counting, these final state interactions have to be incorporated in a well defined manner. ii) The choice of the subtraction points: In principle, a dispersion relation can be subtracted at any point. However, since the amplitude is approximated by a polynomial near these points, they should lie as far as possible from kinematical singularities. Furthermore, we expect that the low energy expansion is more reliable, if the invariant mass of the interacting pion pair is as small as possible at the subtraction points. However, as soon as $I=2$ (and $I=1$) final state interactions are included, the problem depends on two variables s_a and s_b, i.e. the pions interact also in the s_b- and s_c -channels. This is reflected by the fact that there are three dispersion integrals. They should all be subtracted at small momenta, but there is no point in the Mandelstam plane where all three variables s_a, s_b and s_c are small. iii) The subtraction constants as determined from the existing one- loop calculation will have uncertainties due to yet unknown higher order effects. These uncertainties can be estimated by comparing the one-loop amplitude with the leading order term. A precise description of our estimate will be given in section 5.

The solution to the first two problems is straightforward and motivated by the following observation. In chiral perturbation theory, the imaginary part of the $\eta\to 3\pi$ one-loop amplitude is generated by the graphs where $\pi\pi$, $\pi\eta$, $K\bar{K}$ or $\eta\eta$ rescatter. They are easily obtained from two-body unitarity provided the lowest order vertices are inserted in the unitarity relation. Given the absorptive parts, the real part at order p^4 can be reconstructed from a dispersion representation up to a second order polynomial in s_a,s_b,s_c. Due to the work of Gasser and Leutwyler [5], this polynomial is known in terms of m_π, m_K, m_η, F_π, F_K and the low-energy constant L_3.

The Khuri-Treiman equations are of course more general than this dispersion representation of the $\eta\to 3\pi$ amplitude to order p^4. However, they can be matched onto the ChPT one-loop amplitude in the following sense. Consider an iterative solution of eqs. (2.46 - 2.49). In particular, use the current algebra result, $F(s_a,s_b,s_c)^{(0)}=T(s_a)$, as a first approximation to be inserted on the right hand

side of eq. (2.47) and the partial waves of the $\pi\pi$ scattering amplitude as given by their low energy expansion, i.e.

$$f_l^I(s) = e^{i\delta_l^I(s)} \sin\delta_l^I(s) \approx \delta_l^{I,\mathrm{ChPT}}(s) \tag{3.2}$$

where $\delta_l^{I,\mathrm{ChPT}}(s)$ are the expressions for the phaseshifts at leading order ChPT given in Ref. [5]. By construction, the first step of this iteration yields exactly the imaginary parts of the ChPT one-loop amplitude which are due to $\pi\pi$ intermediate states [5]. Moreover, the dispersive part of the Khuri-Treiman equations contains also *all* $\pi\pi$-threshold effects present in the ChPT one-loop amplitude. Therefore, after the first iteration step as described above, we have reproduced all singularities close to the physical region. We note already at this point that three subtractions will be necessary in order to make this procedure well defined.

In the low energy region, the remainder of the ChPT one-loop amplitude can be expanded to a very good accuracy into a polynomial of second order in s_a, s_b, s_c. This last step then determines the subtraction polynomial of the generalized Khuri-Treiman equations.

Before turning to the details of our subtraction prescription, we give a more complete discussion of the structure of the one-loop amplitude in Chiral Perturbation Theory.

3.1 Structure of the ChPT one-loop amplitude

We work with the reduced amplitude $\bar{A}$ defined in eq. (3.1). The aim is to rewrite $A^{1-\mathrm{loop}}(s_a, s_b, s_c)$ as a suitable dispersion integral. The singularities of the amplitude $\bar{A}$ are contained in the unitarity corrections $\mathcal{U}(s_a, s_b, s_c)$. We may split them up further by writing

$$\mathcal{U}(s_a, s_b, s_c) = \mathcal{U}_{\pi\pi}^{\mathrm{disp}}(s_a, s_b, s_c) + \mathcal{U}^{\mathrm{rem}}(s_a, s_b, s_c), \tag{3.3}$$

with

$$\begin{aligned}
\mathcal{U}_{\pi\pi}^{\mathrm{disp}}(s_a, s_b, s_c) \;=\; & \frac{1}{3}\tilde{\Delta}_{0,\pi\pi}(s_a)\,[3T(s_a) + T(s_b) + T(s_c)] \\
& + \frac{1}{2}\tilde{\Delta}_{1,\pi\pi}(s_b)\,[T(s_a) - T(s_c)] + \frac{1}{2}\tilde{\Delta}_{1,\pi\pi}(s_c)\,[T(s_a) - T(s_b)] \\
& + \frac{1}{2}\tilde{\Delta}_{2,\pi\pi}(s_b)\,[T(s_a) + T(s_c)] + \frac{1}{2}\tilde{\Delta}_{2,\pi\pi}(s_c)\,[T(s_a) + T(s_b)] \\
& - \frac{1}{3}\tilde{\Delta}_{2,\pi\pi}(s_a)\,[s_b(t) + T(s_c)]
\end{aligned} \tag{3.4}$$

and

$$\tilde{\Delta}_{I,\pi\pi}(s) = \frac{s^2}{\pi}\int_{4m_\pi^2}^{\infty} ds' \frac{\delta^{I,\mathrm{ChPT}}(s')}{s'^2(s' - s - i\epsilon)}. \tag{3.5}$$

[5] The absorptive parts due to $\pi\eta$, $K\bar{K}$ or $\eta\eta$ intermediate states were not included in the calculation of the imaginary part. Because of their high thresholds, we expect a small effect and will neglect them.

The phaseshifts $\delta^{I,\mathrm{ChPT}}$ are the expressions to leading order in ChPT given in Ref. [5]. $U^{\mathrm{disp}}_{\pi\pi}$ contains the singularities due to $\pi\pi$ intermediate states. The remainder, U^{rem}, is polynomial except for singularities due to $\pi\eta$, $K\bar{K}$ or $\eta\eta$ intermediate states. More explicitly, it is given by

$$\begin{aligned}\mathcal{U}^{\mathrm{rem}}(s_a,s_b,s_c) &= \frac{1}{3}\bar{\Delta}_0(s_a)\left[3T(s_a)+T(t)+T(s_c)\right]\\ &+\frac{1}{2}\bar{\Delta}_1(s_b)\left[T(s_a)-T(s_c)\right]+\frac{1}{2}\bar{\Delta}_1(s_c)\left[T(s_a)-T(s_b)\right]\\ &+\frac{1}{2}\bar{\Delta}_2(s_b)\left[T(s_a)+T(s_c)\right]+\frac{1}{2}\bar{\Delta}_2(s_c)\left[T(s_a)+T(s_b)\right]\\ &+\bar{\Delta}_3(s_a) \qquad (3.6)\end{aligned}$$

with

$$\begin{aligned}\bar{\Delta}_0(s) &= \frac{1}{F_\pi^2}\left\{m_\pi^2 k_{\pi\pi}-(2k_{\pi\pi}-\frac{1}{192\pi^2})s\right\}\\ \bar{\Delta}_1(s) &= \frac{1}{F_\pi^2}\left\{-\frac{1}{3}k_{\pi\pi}+sm^r_{KK}(s)\right\}\\ \bar{\Delta}_2(s) &= \frac{1}{F_\pi^2}\left\{-2m_\pi^2 k_{\pi\pi}+(k_{\pi\pi}+\frac{1}{96\pi^2})s\right\}\\ &+\frac{(3s-4m_K^2)}{4F_\pi^2}J^r_{KK}(s)+\frac{m_\pi^2}{3F_\pi^2}J^r_{\pi\eta}(s)\\ \bar{\Delta}_3(s_a) &= \frac{1}{F_\pi^2}\left\{-\frac{1}{3}(T(s_b)+T(s_c))\left[-2m_\pi^2 k_{\pi\pi}+(k_{\pi\pi}+\frac{1}{96\pi^2})s_a\right]\right\}\\ &-\frac{s_a(3s_a-4m_\pi^2)}{4F_\pi^2(m_\eta^2-m_\pi^2)}J^r_{KK}(s_a)+\frac{m_\pi^2(3s_a-4m_\pi^2)}{3F_\pi^2(m_\eta^2-M\pi^2)}J^r_{\pi\eta}(s_a)\\ &-\frac{m_\pi^2}{2F_\pi^2}J^r_{\eta\eta}(s_a)-\frac{3s_a(3s_a-4m_K^2)}{8F_\pi^2(s_a-4m_K^2)}\left[\bar{J}_{KK}(s_a)-\frac{1}{8\pi^2}\right]. \qquad (3.7)\end{aligned}$$

The functions k_{PP}, J^r_{PQ}, $\bar{J}_{PQ}$ and M^r_{PQ} are defined in Ref. [13] and are not displayed here explicitely; when not given, their arguments are as on the left hand sides of the equations. $\mathcal{U}^{\mathrm{disp}}_{\pi\pi}(s_a,s_b,s_c)$ will be reproduced by iterating the Khuri-Treiman equations as discussed before and shown in more detail below. In fact, it is uniquely determined by unitarity. The rest of the amplitude,

$$\begin{aligned}\bar{A}^{\mathrm{rem}}(s_a,s_b,s_c) &= \bar{A}(s_a,s_b,s_c)-\mathcal{U}^{\mathrm{disp}}_{\pi\pi}(s_a,s_b,s_c)\\ &= T(s_a)+\mathcal{V}(s_a)+\mathcal{W}(s_a,s_b,s_c)+\mathcal{U}^{\mathrm{rem}}(s_a,s_b,s_c) \qquad (3.8)\end{aligned}$$

is smooth in the physical region and it is expanded in a second order polynomial in s_a, s_b, s_c around the center of the Dalitz plot, $s_a = s_b = s_c = s_0 = \frac{1}{3}(m_\eta^2+3m_\pi^2)$:

$$\bar{A}^{\mathrm{rem}}(s_a,s_b,s_c) = \bar{\alpha}+\bar{\beta}(s_a-s_0)+\bar{\gamma}(s_a-s_0)^2+\bar{\delta}(s_b-s_c)^2. \qquad (3.9)$$

This form is the most general second order polynomial if the constraint $s_a+s_b+s_c = 3s_0 = \frac{1}{3}(m_\eta^2+3m_\pi^2)$ and bose symmetry are satisfied. The expansion of $\mathcal{U}^{\rm rem}$ is tedious and its analytic form will not be displayed here. $T(s_a), \mathcal{V}(s_a)$ and $\mathcal{W}(s_a,s_b,s_c)$ are already polynomial and their contribution to $\bar{\alpha}$, ..., $\bar{\delta}$ is

$$\begin{aligned}
\bar{\alpha} &= T(s_0)+\mathcal{V}(s_0)+\mathcal{W}(s_0,s_0,s_0) \\
\bar{\beta} &= \frac{3}{(m_\eta^2-m_\pi^2)}\{1+a_1+3a_2(m_\eta^2-m_\pi^2)+a_3(9m_\eta^2-m_\pi^2) \\
&\quad +\frac{2}{3}(d_1+\frac{4m_\pi^2}{(m_\eta^2-m_\pi^2)}\,d_2)\}-\frac{12s_0}{F_\pi^2(m_\eta^2-m_\pi^2)}L_3 \\
\bar{\gamma} &= \frac{6}{F_\pi^2(m_\eta^2-m_\pi^2)}L_3 \\
\bar{\delta} &= -\frac{2}{F_\pi^2(m_\eta^2-m_\pi^2)}L_3. \qquad (3.10)
\end{aligned}$$

The constants a_1, a_2, a_3, d_1 and d_2 are tabulated in Ref. [5]. We note here that the coefficients $\bar{\beta}$, $\bar{\gamma}$ and $\bar{\delta}$ depend on the low energy constant L_3 which is phenomenologically not known very accurately [6]. Its value extracted from K_{l4} decays is [35]

$$L_3 = (-3.62 \pm 1.31)\cdot 10^{-3}. \qquad (3.11)$$

The error bar on L_3 leads to corresponding error bars on $\bar{\beta}$, $\bar{\gamma}$ and $\bar{\delta}$:

$$\begin{aligned}
\Delta_{|_{L_3}}\bar{\alpha} &= 0 \\
\Delta_{|_{L_3}}\bar{\beta} &= -\frac{12s_0}{F_\pi^2(m_\eta^2-m_\pi^2)}(\Delta L_3) \approx \mp 0.76\,\mathrm{GeV}^{-2} \\
\Delta_{|_{L_3}}\bar{\gamma} &= \frac{6}{F_\pi^2(m_\eta^2-m_\pi^2)}(\Delta L_3) \approx \pm 3.18\,\mathrm{GeV}^{-4} \\
\Delta_{|_{L_3}}\bar{\delta} &= -\frac{2}{F_\pi^2(m_\eta^2-m_\pi^2)}(\Delta L_3) \approx \mp 1.06\,\mathrm{GeV}^{-4} \qquad (3.12)
\end{aligned}$$

We shall comment on the importance of this uncertainty in the determination of L_3 in section 5 where we discuss the phenomenological implications of our results.

The information needed to fix the subtraction constants of the generalized Khuri-Treiman equations is contained in coefficients $\bar{\alpha}$, ..., $\bar{\delta}$, eq. (3.10), as well as in the corresponding expressions coming from the expansion of $\mathcal{U}^{\rm rem}$.

3.2 Fixing the subtraction constants

We consider the generalized Khuri-Treiman equations in the three times subtracted form given in eqs. (2.46)-(2.49) [7]. The s_1, s_2,... w_2 are finite subtraction points,

[6] Note that L_3 is scale independent.

[7] Note the functions U, V, W are not identical to the functions $\mathcal{U}$, etc. introduced above.

$f_l^I = \sin\delta_l^I e^{i\delta_l^I}$ is the partial wave for $\pi\pi$ scattering with angular momentum l in the isospin channel I and the precise definition of $\tilde{F}$ and $\bar{F}$ has been given in section 2. P is a polynomial of second order in s_a, s_b, s_c with the same form as eq. (3.9):

$$P(s_a, s_b, s_c) = \alpha + \beta s_a + \gamma s_a^2 + \delta(s_b - s_c)^2. \tag{3.13}$$

The reason for using three subtractions will become clear soon. Note that the polynomial P is not equal to $\bar{A}^{\rm rem}$ because the latter refers to a twice subtracted dispersion relation (see eq. (3.5)) while P corresponds to three subtractions.

Now we iterate eq. (2.47) by inserting on the right hand side the current algebra expression $F(s_a, s_b, s_c) = T(s_a)$. Moreover, we replace f_l^I by its low energy expansion

$$f_l^I(s_a) \approx \delta_l^{I,\rm ChPT}(s_a). \tag{3.14}$$

We observe that this reproduces the absorptive parts of the ChPT one-loop amplitude due to $\pi\pi$ intermediate states. For isospin $I = 0, 2$ this is trivial because $T(s_a)$ is linear in s_a and hence $T(s_b) + T(s_c)$ is again a first order polynomial in s_a. For the $I = 1$ p-wave $\pi\pi$ intermediate state the absorptive part is in general given by

$$\mathrm{Im}F(s_a, s_b, s_c)_{|_{\delta_1^1}} = e^{i\delta_1^1(s_b)} \sin\delta_1^1(s_b) \frac{3(s_c - s_a)}{2K(s_b)} F_1^{s_a}(s_b) + (t \leftrightarrow s_c) \tag{3.15}$$

where $K(s_b)$ is the Kacser function and $F_1^{s_a}(s_b)$ is the p-wave projection in the s_b-channel of the function $F(s_a, s_b, s_c)$ defined in section 2. Setting $T(s_a) = a + bs_a$, the p-wave projection in the s_b-channel is calculated to be

$$T_1^{s_a}(s_b) = -\frac{1}{3} K(s_b) b. \tag{3.16}$$

Thus the first iteration with the approximations given above yields

$$\mathrm{Im}F(s_a, s_b, s_c)_{|_{\delta_1^1}} = \delta_1^{1,\rm ChPT} \frac{1}{2}(T(s_a) - T(s_c)) + (s_b \leftrightarrow s_c). \tag{3.17}$$

This is indeed the result of the one-loop calculation obtained in Ref. [5].

Turning now to the dispersive part, we shall show how the real part of $\mathcal{U}_{\pi\pi}^{\rm disp}$, eq. (3.4), is reproduced in the first iteration of the generalized Khuri-Treiman equations. In order to make the argument more transparent, let us consider first the simpler case where all subtractions are taken at zero. The term $U(s_a)$ on the right hand side of eq. (2.46) then reads, after the first iteration

$$\mathrm{Re}\, U^{\rm iter}(s_a) = \frac{s^3}{\pi} P \int_{4m_\pi^2}^{\infty} ds' \frac{\delta_0^{0,\rm ChPT}(s')(\hat{a} + \hat{b}s') - \delta_0^{2,\rm ChPT}(\bar{a} + \bar{b}s')}{s'^3(s' - s_a - i\epsilon)} \tag{3.18}$$

with

$$\begin{aligned} \hat{a} &= \frac{5}{3}a + bs_0, & \hat{b} &= \frac{2}{3}b \\ \bar{a} &= \frac{2}{3}a + bs_0, & \bar{b} &= -\frac{1}{3}b \end{aligned} \tag{3.19}$$

and

$$a = 1 - \frac{3s_0}{m_\eta^2 - m_\pi^2}, \qquad b = \frac{3}{m_\eta^2 - m_\pi^2}. \tag{3.20}$$

In eq. (3.18), P denotes the principal value of the integral; the combinations in eq. (3.19) simply stand for the appropriate isospin projections. Using the decomposition

$$\frac{s^3}{\pi} P \int ds' \frac{\delta^I(s')(s'-z)}{s'^3(s'-s-i\epsilon)} = (s-z)\frac{s^2}{\pi} P \int ds' \frac{\delta^I(s')}{s'^2(s'-s-i\epsilon)} + z\frac{s^2}{\pi} P \int ds' \frac{\delta^I(s')}{s'^3} \tag{3.21}$$

eq. (3.18) can be brought into the form

$$\begin{aligned} \mathrm{Re}\, U^{\mathrm{iter}}(s_a) &= \left[T(s_a) + \frac{1}{3}(T(s_b)+T(s_c))\right] \mathrm{Re}\tilde{\Delta}_{0,\pi\pi}(s_a) \\ &\quad -\hat{a}\frac{s_a^2}{\pi} P \int ds' \frac{\delta_0^{0,\mathrm{ChPT}}(s')}{s'^3} \\ &\quad -\frac{1}{3}\left[T(s_a)+T(s_c)\right] \mathrm{Re}\tilde{\Delta}_{2,\pi\pi}(s_a) \\ &\quad +\bar{a}\frac{s^2}{\pi} P \int ds' \frac{\delta_0^{2,\mathrm{ChPT}}(s')}{s'^3}. \end{aligned} \tag{3.22}$$

We thus have transformed $\mathrm{Re}\, U^{\mathrm{iter}}(s)$ into the first and last term of $\mathcal{U}_{\pi\pi}^{\mathrm{disp}}$ plus two polynomial terms. In other words, eq. (3.21) serves to transform a three times subtracted relation into a twice subtracted one. Likewise, we may decompose

$$\begin{aligned} \mathrm{Re}\left(V(s_b)+V(s_c)\right)^{\mathrm{iter}} &= \frac{1}{2}\left[T(s_a)+T(s_c)\right] \mathrm{Re}\tilde{\Delta}_{2,\pi\pi}(s_b) \\ &\quad -\tilde{a}\frac{s_b^2}{\pi} P \int ds' \frac{\delta_0^{2,\mathrm{ChPT}}(s')}{s'^3} + (s_b \leftrightarrow s_c) \end{aligned} \tag{3.23}$$

with

$$\tilde{a} = a + \frac{3}{2} b s_0. \tag{3.24}$$

Finally, using (3.16) and the definition of $\hat{F}(s')$, eq. (2.44), we see that the $I=1$ contribution in the generalized Khuri-Treiman equations yields precisely the terms in proportion to $\tilde{\Delta}_{1,\pi\pi}$ in eq. (3.4):

$$\mathrm{Re}\left((s_a-s_c)W(s_b)+(s_a-s_b)W(s_c)\right)^{\mathrm{iter}} = \frac{1}{2}\left[T(s_a)-T(s_c)\right] \mathrm{Re}\tilde{\Delta}_{1,\pi\pi}(s_b) + (s_b \leftrightarrow s_c). \tag{3.25}$$

We see that linking the dispersion technique to the one-loop ChPT calculation allows to subtract U,V and W separately avoiding the problem (mentioned previously) that these points may lie outside the physical region.

We are now ready to determine the subtraction polynomial P of the triple subtracted Khuri-Treiman equations. After the first iteration, the amplitude can be written as

$$F(s_a,s_b,s_c)^{\mathrm{iter}} = P(s_a,s_b,s_c) + \mathcal{U}_{\pi\pi}^{\mathrm{disp}}(s_a,s_b,s_c) + R(s_a,s_b,s_c). \tag{3.26}$$

If all subtractions are taken at zero, R is given by eqs. (3.22)- (3.23), i.e.

$$\begin{aligned} R(s_a,s_b,s_c) &= -\hat{a}\frac{s_a^2}{\pi}P\int ds' \frac{\delta_0^{0,\mathrm{ChPT}}(s')}{s'^3} \\ &\quad + \left(\bar{a}\frac{s_a^2}{\pi} - \tilde{a}\frac{s_b^2+s_c^2}{\pi}\right) P\int ds' \frac{\delta_0^{2,\mathrm{ChPT}}(s')}{s'^3}. \end{aligned} \tag{3.27}$$

Requiring the matching of the first iteration of the generalized Khuri-Treiman equations with the one-loop amplitude from ChPT we obtain

$$\begin{aligned} P(s_a,s_b,s_c) &= \left\{\bar{A}(s_a,s_b,s_c) - \mathcal{U}_{\pi\pi}^{\mathrm{disp}} - R(s_a,s_b,s_c)\right\}_{\mathrm{expand}} \\ &= \bar{\alpha} + \bar{\beta}(s_a-s_0) + \bar{\gamma}(s_a-s_0)^2 + \bar{\delta}(s_b-s_c)^2 - R(s_a,s_b,s_c) \end{aligned} \tag{3.28}$$

where the subscript "expand" means a Taylor expansion up to second order in s_a, s_b, s_c; in fact the expression in the curly brackets is just $\bar{A}^{\mathrm{rem}} - R$.

Eq. (3.28) and its generalization for finite subtractions points described below is the main result of this section. It describes our method of using the ChPT one-loop amplitude (see however below) to fix the subtraction constants of the generalized Khuri-Treiman equations. In order to make the procedure transparent, that is show explicitely how the higher corrections unitarize the amplitude, we were forced to subtract the Khuri-Treiman equations three times. Otherwise the integrals occuring in $R(s_a,s_b,s_c)$ would not converge. By construction, the first step in an iteration of the Khuri-Treiman equations reproduces the ChPT one-loop result in the physical decay region to very good accuracy. The numerical solution of the generalized Khuri-Treiman equations as attempted in section 4 can therefore be interpreted as a correction on top of the ChPT one-loop amplitude due to all possible two-body final state interactions of pions.

There remains the important question of higher order corrections to the one-loop results which may shift the subtraction constants substantially. We will address this issue in section 5. Here we only note that also in this case the above framework of three subtractions can be employed if the necessary modifications are made.

3.3 Finite subtraction points

In the preceeding subsection all three subtractions have been taken at zero for the sake of simplicity. Here we shall describe the modifications which arise if the subtractions are taken at finite values. We do this for two reasons: Since the dispersion relations do not fix the subtractions points, varying them over a certain domain gives an estimate of the error of our procedure (see also the discussion in section 5). Second, it is numerically favorable to have subtraction points which do not coincide when we solve the Khuri-Treiman equations iteratively.

Introducing now finite subtraction points and performing essentially the same steps as before, we find that only the function $R(s_a,s_b,s_c)$ is modified. It explicitly

depends on subtraction points s_i, v_i, i=1,2,3 and w_i, i=1,2 and is given as

$$\begin{aligned} R(s_a,s_b,s_c;s_i) &= \hat{b}R^{(0)}(s_a;s_1,s_2,s_3;-\frac{\hat{a}}{\hat{b}}) - \bar{b}R^{(2)}(s_a;v_1,v_2,v_3;-\frac{\bar{a}}{\bar{b}}) \\ &+\check{b}R^{(2)}(s_b;v_1,v_2,v_3;-\frac{\check{a}}{\check{b}}) + \tilde{b}R^{(2)}(s_c;v_1,v_2,v_3;-\frac{\tilde{a}}{\tilde{b}}) \\ &+bR^{(1)}(s_a,s_b,s_c;w_1,w_2). \end{aligned} \tag{3.29}$$

The explicit form of functions $R^{(I)}$, $I=0,1,2$ is given in Appendix D.

The subtraction polynomial is then again given by eq. (3.28) with R taken from (3.29). It depends explicitly on the subtraction points s_i, v_i and w_i. However, by construction this dependence on the subtraction points is counterbalanced by a corresponding dependence of the dispersive part of the generalized Khuri-Treiman equations, provided only the first step of the iteration described above is performed. The procedure of fixing subtraction constants is in this sense independent on the choice of the subtraction points. Up to the first iteration, the ChPT one-loop amplitude is reproduced, in the physical region, for any value s_1, ..., w_2 in the low energy regime. Beyond the first iteration this is no longer true.

Finally we give numerical values for coefficients α, ..., δ of the subtraction polynomial P. We consider the sets of subtraction points $SP = s_1 = v_1 = w_1, s_2 = v_2 = w_2, s_3 = v_3$ displayed in Table 1. The input parameters we use are $m_\pi = 140\text{MeV}$, $m_\eta = 549\text{MeV}$, $F_\pi = 92.4\text{MeV}$, $F_K = 114\text{MeV}$, $L_3 = (-3.62 \pm 1.31)10^{-3}$. The calculated coefficients α, ..., δ for these sets of subtraction points are given in Table 2.

The dependence on the choice of subtraction points is substantial and we shall discuss how it propagates into the final numerical solution in section 5. Note that error bars due to the uncertainty in the determination of L_3 are correlated. For instance, the value of $P(s_a,s_b,s_c)$ at the center of the Dalitz plot does not depend on L_3 – the errors for α, ..., δ cancel for this quantity. Also it appears that for subtraction points $SP \approx 0$, γ is rather small. In the physical region, the term in proportion to γ contributes only $\approx 2\%$ to the subtraction polynomial. The error bar on γ due to the uncertainty in L_3 is therefore phenomenologically less important.

3.4 Comments

We have swept over several subtle points rather briskly and would like to come back to them.

1. The polynomial P depends on four constants. On the other hand, we have subtracted the three functions U, V and W separately; this implies 3+3+2 = 8 constants. It is clear from the form of P that there are only four physically relevant parameters and that there are redundant parameters. The reason for this is found in a general invariance of the dispersion relations: they fix a function only up to a polynomial; therefore, we can 'shift' certain constants

from one function to the other. For instance, we can redefine in this way two constants in W and two in V (the constant and the linear terms). Thus, only four constants remain.

2. The asymptotic behaviour of the amplitude has been discussed only briefly. Taking three subtractions we want to make sure that the actual behaviour in the asymptotic region does not matter for the solution in the physical decay region. There is however an other subtlety which we should mention. Mathematically speaking, the solution to the integral equations (2.46-2.51) is not completely determined by specifying the asymptotic behaviour of the amplitude. The number of parameters (extracted from ChPT) to be input depends also on the asymptotic behaviour of the $\pi\pi$-phase shift. [8] Let us consider the twice subtracted relation for definiteness and omit V and W. The solution to this problem can be written in the form

$$F(s) = P(s) + \Phi_{10}(s) + \psi_0(s) \tag{3.30}$$

where Φ_{10} and ψ_0 are defined in eqs. (4.8-4.15). Now, if the phase goes to zero for large s, the Omnes factor is constant; correspondingly, the amplitude rises linearly with s. On the other hand, if the phase approaches π, the Omnes factor decays like s^{-1} and the amplitude tends towards a constant. Stated differently, a given asymptotic behaviour of the amplitude, say $\sim$ const., requires one or two subtractions for the two limiting cases of the phase shift respectively. This ambiguity in the phase is reflected in an additional term

$$\frac{Q(s)}{D(s)}(s-s_1)(s-s_2)(s-s_3), \qquad Q(s) \text{ polynomial}, \tag{3.31}$$

which can be added to the approximate solution Φ_{10}, c.f. eq. (4.21). It introduces an uncertainty in the final solution which should be well controlled since the assumptions entering the analysis are not rigorous. We have estimated this uncertainty by modelling the phase in the high energy region. The details as well as the resulting error bars on our final answer are given in section 5.

4 The iteration

With reasonable assumptions we now build up an iterative scheme for the numerical solution of the set of coupled equations for the projected amplitudes U, V, W. It consists of two distinct kinds of iterations. The first one accumulates contributions to V and W for a corresponding part of U while the second yields the contributions to U itself.

[8] We are indebted to H. Leutwyler for pointing out this to us. A more complete discussion of these issues can be found in Ref. [22].

4.1 Iterating in f_0^2 and f_1^1

The first type of iteration relies on the assumption that to lowest order only U contributes, but not V and W. It is motivated by the fact that pion-pion scattering at low energies is dominated by the s-wave, $I = 0$ channel as the s-wave, $I = 2$ contribution is suppressed by a much smaller phase shift $f_0^2 \ll f_0^0$. The $I = 1$ contribution comes from a p-wave scattering and therefore is also suppressed. We may thus expect that, in comparison to V and W, U will still yield the dominant contribution to F in our refined analysis.

To organize this first iteration we take the terms with the phase shifts f_0^2, f_1^1 as perturbations and introduce accordingly a counting parameter λ. f_0^0 is taken to be of $O(\lambda^0)$ whereas

$$\begin{aligned} f_0^2 &\to \lambda f_0^2 \\ f_1^1 &\to \lambda f_1^1 \end{aligned} \tag{4.1}$$

are treated as small parameters. In principle, one could introduce different counting parameters for the two isospin channels, but for sufficently many iterations in λ, this is irrelevant. Expansion of V, W and U in a series in λ yields

$$\begin{aligned} V(s_a) &= \sum_0^\infty \lambda^k V_k(s_a) \\ W(s_a) &= \sum_0^\infty \lambda^k W_k(s_a) \\ U(s_a) &= \sum_0^\infty \lambda^k U_k(s_a) \end{aligned} \tag{4.2}$$

where we set by assumption $V_0(s_a) = W_0(s_a) = 0$. We insert these expansions in the integral equations eqs. (2.52), (2.53) and (2.54) and obtain by equating equal powers of λ

$$\begin{aligned} V_k(s_a) &= \frac{\prod_{i=1}^3 (s_a - s_i)}{\pi} \int_4^\infty \frac{ds'_a}{\prod_{j=1}^3 (s'_a - s_j)(s'_a - s_a - i\varepsilon)} \\ &\quad \cdot f_0^{2*}(s'_a) \left[\tilde{P}(s'_a)\delta_{k1} + \overline{U}_{k-1}(s'_a) + V_{k-1}(s'_a) \right. \\ &\quad \left. + \overline{V}_{k-1}(s'_a) + \overline{(s_a - s_c) W_{k-1}}\,(s'_a) \right], \end{aligned} \tag{4.3}$$

$$\begin{aligned} W_k(s_a) &= \frac{(s_a - s_1)(s_a - s_2)}{3\pi} \int_4^\infty \frac{ds'_a}{(s'_a - s_1)(s'_a - s_2)(s'_a - s_a - i\varepsilon)} \\ &\quad \cdot f_1^{1*}(s'_a) \left[\hat{P}(s'_a)\delta_{k1} \right. \\ &\quad + \frac{3}{4K^2(s'_a)} \{ \overline{(s_c - s_b) U_{k-1}}\,(s'_a) + \overline{(s_b - s_c) V_{k-1}}\,(s'_a) \\ &\quad \left. + \overline{(s_b - s_c)^2} \cdot W_{k-1}(s'_a) + \overline{(s_b - s_c)(s_a - s_c) W_{k-1}}\,(s'_a) \} \right] \\ &\quad + \text{perm.} \end{aligned} \tag{4.4}$$

and

$$U_k(s_a) = \Phi_{0k}(s_a) + \frac{\prod_{i=1}^3(s_a - s_i)}{\pi}\int_4^\infty \frac{ds'_a}{\prod_{j=1}^3(s'_a - s_j)(s'_a - s_a - i\varepsilon)} \cdot f_0^{0*}(s'_a)\,[U_k(s'_a) + \frac{2}{3}\overline{U}_k(s'_a)], \tag{4.5}$$

where we have introduced the subtraction functions

$$\begin{aligned}\Phi_{0k}(s_a) \equiv\ & \frac{\prod_{i=1}^3(s_a - s_i)}{\pi}\int_4^\infty \frac{ds'_a}{\prod_{j=1}^3(s'_a - s_j)(s'_a - s_a - i\varepsilon)} \\ & \cdot\{f_0^{0*}(s'_a)\,[\{\overline{P}(s'_a) + \frac{2}{3}\tilde{P}(s'_a)\}\delta_{k0} + \frac{2}{3}V_k(s'_a) \\ & + \frac{8}{3}\overline{V}_k(s'_a) + \frac{4}{3}\overline{(s_c - s_a)W_k}\,(s'_a)] \\ & - f_0^{2*}(s'_a)\,[\frac{2}{3}\tilde{P}(s'_a)\delta_{k1} + \frac{2}{3}\overline{U}_{k-1}(s'_a) + \frac{2}{3}V_{k-1}(s'_a) \\ & + \frac{2}{3}\overline{V}_{k-1}(s'_a) + \frac{2}{3}\overline{(s_a - s_c)W_{k-1}}\,(s'_a)]\}.\end{aligned} \tag{4.6}$$

It is now obvious that for given $U_{k-1}, V_{k-1}, W_{k-1}$ and their respective projections we may use eqs. (4.3)-(4.4) to determine V_k and W_k. This allows to compute the subtraction function Φ_{0k} as given in eq. (4.6). If we can also solve eq. (4.5) for U_k, the iteration step is complete and we may perform it once again for k instead of $k-1$. Note that the lowest non-vanishing contributions U_0, V_1 and W_1 are completely determined by the different projections of the subtraction polynomial P containing the input information of ChPT on the decay amplitude.

As the process converges rapidly, we will have to perform a small number of iterations, typically four or five, to obtain a precision below one part in thousand. Of course we take now $\lambda = 1$ as it was introduced as a counting parameter only and may sum the different contributions to obtain the fully iterated U, V and W.

4.2 Iterating in f_0^0

We turn to the second kind of iteration which yields the yet undetermined U_k from eq. (4.5). We thereby follow the discussion of Bronzan [29] and Neveu and Scherk [31] extending it to our case. As we are dealing with one variable only we omit the usual subscripts here.

If in the equation (4.5) for U_k the second term in the square bracket were absent, we would have to deal with an Omnès type of integral equation describing ordinary two pion-pion rescattering without rediffusion terms coming from the third pion in the final state. Decomposing U_k into two auxiliary functions

$$U_k(s) \equiv \Phi_{1k}(s) + \psi_k(s) - \frac{2}{3}\overline{U}_k(s) \tag{4.7}$$

where Φ_{1k} collects the two pion-pion rescattering contributions and $\psi_k - \frac{2}{3}\overline{U}_k$ the rediffusion effects we are able to recast the equation for U_k in a form which is now accessible for a second kind of iteration [29, 31].

By its definition Φ_{1k} fulfils the Omnès integral equation

$$\begin{aligned}\Phi_{1k}(s) \equiv \Phi_{0k}(s) + \frac{\prod_{i=1}^{3}(s-s_i)}{\pi}\int_4^\infty \frac{ds'}{\prod_{j=1}^{3}(s'-s_j)(s'-s-i\varepsilon)} \\ \cdot f_0^{0*}(s')\,\Phi_{1k}(s)\end{aligned} \tag{4.8}$$

which is indeed solvable in terms of Φ_{0k} [36] and yields

$$\begin{aligned}\Phi_{1k}(s) = \Phi_{0k}(s) + \frac{\prod_{i=1}^{3}(s-s_i)}{\pi D(s_+)}\int_4^\infty \frac{ds'}{\prod_{j=1}^{3}(s'-s_j)(s'-s-i\varepsilon)} \\ \cdot f_0^{0}(s')D(s'_+)\,\Phi_{0k}(s')\end{aligned} \tag{4.9}$$

where the solution is determined only up to a polynomial which we will explicitely introduce and discuss below. Here $s_\pm = s \pm i\varepsilon$ and $D(s)$ is the usual Omnès function corresponding to the phase shift δ_0^0

$$D(z) = e^{-\frac{1}{\pi}\int_4^\infty ds' \frac{\delta_0^0(s')}{s'-z}}. \tag{4.10}$$

As its the discontinuity is given by

$$D(s_+) - D(s_-) = -2iD(s_+)f_0^0(s) = -2iD(s_-)f_0^{0*}(s) \tag{4.11}$$

we may represent it as a dispersion integral

$$D(z) = -\frac{1}{\pi}\int_4^\infty ds' \frac{D(s'_+)f_0^0(s')}{s'-z}. \tag{4.12}$$

This representation and the insertion of the dispersion representation eq. (4.6) for Φ_{0k} into the formula (4.9) allows us to eliminate Φ_{0k} in the latter and to rewrite Φ_{1k} in the more convenient form

$$\begin{aligned}\Phi_{1k}(s) = \frac{\prod_{i=1}^{3}(s-s_i)}{\pi D(s_+)}\int_4^\infty \frac{ds'}{\prod_{j=1}^{3}(s'-s_j)(s'-s-i\varepsilon)} \\ \cdot D(s'_-)\{f_0^{0*}(s')\,[\{\overline{P}(s') + \frac{2}{3}\check{P}(s')\}\delta_{k0} + \frac{2}{3}V_k(s') \\ + \frac{8}{3}\overline{V}_k(s') + \frac{4}{3}\overline{(s_c-s_a)W_k}\,(s')] \\ - f_0^{2*}(s')\,[\frac{2}{3}\check{P}(s')\delta_{k1} + \frac{2}{3}\overline{U}_{k-1}(s') + \frac{2}{3}V_{k-1}(s') \\ + \frac{2}{3}\overline{V}_{k-1}(s') + \frac{2}{3}\overline{(s_a-s_c)W_{k-1}}\,(s')]\}.\end{aligned} \tag{4.13}$$

To obtain the desired form of the equation for U_k accessible to an iterative solution we next insert eqs. (4.6) and (4.8) into the r.h.s. of (4.5) and find that ψ_k obeys

$$\psi_k(s) = \frac{2}{3}\overline{U}_k(s) + \frac{\prod_{i=1}^3(s-s_i)}{\pi}\int_4^\infty \frac{ds'}{\prod_{j=1}^3(s'-s_j)(s'-s-i\varepsilon)} \cdot f_0^{0*}(s')\,\psi_k(s). \tag{4.14}$$

This equation is again of the Omnès type and has a solution in terms of the unknown $\overline{U}_k$

$$\psi_k(s) = \frac{2}{3}\overline{U}_k(s) + \frac{\prod_{i=1}^3(s-s_i)}{\pi D(s_+)}\int_4^\infty \frac{ds'}{\prod_{j=1}^3(s'-s_j)(s'-s-i\varepsilon)} \cdot f_0^0(s')D(s'_+)\,\frac{2}{3}\overline{U}_k(s'). \tag{4.15}$$

Insertion of this result into eq. (4.7) yields the desired form of the equation for U_k [29, 31]

$$U_k(s) = \Phi_{1k}(s) + \frac{\prod_{i=1}^3(s-s_i)}{\pi D(s_+)}\int_4^\infty \frac{ds'}{\prod_{j=1}^3(s'-s_j)(s'-s-i\varepsilon)} \cdot f_0^0(s')D(s'_+)\,\frac{2}{3}\overline{U}_k(s'). \tag{4.16}$$

Φ_{1k} is already determined in eq. (4.13) as an Omnès inversion. We may now account for the second term in eq. (4.16) by iteration, noting that at every step one multiplies with the phase shift f_0^0. Introducing the counting parameter μ

$$f_0^0 \to \mu f_0^0 \tag{4.17}$$

we expand U_k in a series in μ

$$U_k(s) = \sum_1^\infty \mu^{m-1}\,\Phi_{mk}(s) \tag{4.18}$$

and obtain for $m > 1$

$$\Phi_{mk}(s) = \frac{\prod_{i=1}^3(s-s_i)}{\pi D(s_+)}\int_4^\infty \frac{ds'}{\prod_{j=1}^3(s'-s_j)(s'-s-i\varepsilon)} \cdot f_0^0(s')D(s'_+)\,\frac{2}{3}\overline{\Phi}_{(m-1)k}(s'). \tag{4.19}$$

Again a small number of iterations is sufficient as the process here converges rapidly, too. Taking now $\mu = 1$, we sum up the different contributions to obtain the fully iterated U_k.

4.3 Explicit form of Φ_{10} and numerical aspects of the iteration

For numerical purposes it is convenient to have an explicit form for Φ_{10} in terms of the subtraction polynomial and the Omnès function only. As for $k = 0$ $D(z)$ is the only function with a cut under the integral (4.13) we may use eq. (4.11) to rewrite $f_0^{0*}(s)D(s_-)$ and recast the dispersion integral along the cut L as a contour integral along C starting at ∞ and going down to 4 lying infinitesimally below the cut L, turning there and going back to ∞ infinitesimally above the real axis such that

$$\begin{aligned}\Phi_{10}(s) &= -\frac{\prod_{i=1}^{3}(s-s_i)}{2i\pi D(s_+)}\int_C \frac{dz'}{\prod_{j=1}^{3}(z'-s_j)(z'-s-i\varepsilon)} \\ &\quad \cdot D(z')\,[\overline{P}(z') + \frac{2}{3}\tilde{P}(z')] \\ &\quad + \prod_{i=1}^{3}(s-s_i)\frac{Q(s)}{D(s)}. \end{aligned} \tag{4.20}$$

$Q(s)$ is the polynomial occuring in the general solution for Φ_{1k} which is not restricted as long as no asymptotic boundary conditions are imposed. The form (4.20) is easily evaluated with the help of the residue calculus and yields after a little algebra the final result

$$\begin{aligned}\Phi_{10}(s) &= [\overline{P}(s) + \frac{2}{3}\tilde{P}(s)] \cdot \frac{1-D(s)}{D(s)} \\ &\quad + [\overline{P}(s_1) + \frac{2}{3}\tilde{P}(s_1)] \cdot \frac{(s-s_2)(s-s_3)}{(s_1-s_2)(s_1-s_3)} \cdot \frac{D(s_1)-1}{D(s)} \\ &\quad + [\overline{P}(s_2) + \frac{2}{3}\tilde{P}(s_2)] \cdot \frac{(s-s_1)(s-s_3)}{(s_2-s_1)(s_2-s_3)} \cdot \frac{D(s_2)-1}{D(s)} \\ &\quad + [\overline{P}(s_3) + \frac{2}{3}\tilde{P}(s_3)] \cdot \frac{(s-s_1)(s-s_2)}{(s_3-s_1)(s_3-s_2)} \cdot \frac{D(s_3)-1}{D(s)} \\ &\quad + \prod_{i=1}^{3}(s-s_i)\frac{Q(s)}{D(s)}. \end{aligned} \tag{4.21}$$

Note that it is of course possible to set two or more of the subtraction points s_i in Φ_{10} equal. As one has then to deal with multiple poles the expression for the corresponding residue becomes more involved.

We finally turn to a short description of the numerical aspects of our iterative scheme for the solution of the set of coupled integral equations for the projected amplitudes U, V and W.

To obtain the decay amplitude with the inclusion of the final state interactions as described by the Khuri-Treiman equation we need to know the three functions $U(z), V(z), W(z)$ only for physical values of z lying infinitesimally above the real axis, $z = s + i\varepsilon$. But in both types of iterations described above, projections of U, V

and W have to be computed. Since the corresponding projection integrals involve contours lying in the complex plane, the functions must be known in a certain domain around the real axis.

As discussed in section 2 there is one s_a-region, namely $(m-1)^2 < s_a < (m+1)^2$, in which the projection integral has to be performed along a contour joining two points lying in the upper and lower complex half planes respectively which must not intersect the real axis from 4 up to ∞ as the integrands have a cut there. As they are analytic elsewhere we are free to choose those paths which minimize the number of necessary lattice points in the complex plane. The two possible choices join the respective end points as given in eq. (2.42) along the path the end points themselves describe as s_a increases from $(m-1)^2$ to $(m+1)^2$. In a second s_a-region with $\frac{m^2-1}{2} < s_a < (m-1)^2$ we have to perform integrals along paths lying infinitesimally above and below the real axis such that we have to know all the functions involved for $z = s - i\varepsilon$ if $4 < s < m+1$.

As we are doing numerical computations, we have to replace the connected domains just discussed by a lattice. The spacing of its points is adapted to the accuracy required and to the possible occurence of numerically problematical points. Of course we will cut off the different integrals at some large value of the integration variable which is determined on one hand by the phenomenological knowledge of the pion scattering phases involved and on the other by demanding that numerical results do not change sensibly if one varies the cut-off. The corresponding cut-off for negative values of s_a is then automatically fixed by eqs. (2.42). As a result we have to know all the functions on a lattice of points lying in the complex plane as displayed in Fig. 2. The actual numbers for the different cut-offs are given in section 5 and their impact on our results is discussed there.

5 Numerical Results

We consider the decay function in the form (see eq. (2.46))

$$\begin{aligned} F(s_a,s_b,s_c) &= P(s_a,s_b,s_c) + U(s_a) + V(s_b) + V(s_c) \\ &\quad + (s_a - s_c)W(s_b) + (s_a - s_b)W(s_c). \end{aligned} \tag{5.1}$$

P is a polynomial and U, V and W correspond to the $I = 0, 2$ and 1 pion rescattering channels. They satisfy the generalized Khuri-Treiman dispersion equations, which describe the unitary corrections to the $\eta \to 3\pi$ decays (see eqs. (2.52,2.53,2.54)). As explained above, we solve the dispersion relation iteratively, starting from an aproximative solution obtained by Neveu and Scherk.

Using the existing one-loop results of Gasser and Leutwyler as basis and casting their unitary corrections into a dispersion relation, we were lead to a three times subtracted dispersion relation for the three amplitudes U, V, W. Although this procedure appears reasonable it is by no means unique. In order to assess it, we consider for comparison also a twice subtracted case where the subtraction polynomial

is simply taken from current algebra.

5.1 Uncertainties

We can identify several sources of uncertainties. Dispersion relations do not fix the subtraction points, except of course for the requirement that they should lie in a region where the approximate theory makes sense. In addition there is the ambiguity to the solution of the Khuri-Treiman equations related to the asymptotic behaviour of the $\pi\pi$-phase shift and the amplitude itself, as discussed in sect. 3. Then, there are the errors in the input parameters (the subtraction constants). The two uncertainties are of course not completely disconnected; for instance the one-loop result from which we determine the subtraction constants may be rather accurate for some values of the subtraction points but not for others, and so a wrong choice of the subtraction point may underestimate the error completely. And finally, there are technical problems, such as the convergence of the iteration and the numerical integration in the complex plane.

1. Varying the subtraction points

In section 3, we constructed the second order subtraction polynomial which was obtained by writing the one-loop result in the form of a three times subtracted dispersion relation. This polynomial then serves as the starting point for the complete dispersion relation. As discussed in section 3, the choice of the three subtraction points s_1, s_2, s_3 for U and those for V and W, which will be denoted collectively by SP, affects the subtraction polynomial considerably and consequently the complete amplitude. Whereas in chiral perturbation theory and in view of the treatment in section 3 small SP (at $s_i \approx 0$) seem most natural, varying the points gives us a feeling for the error. We have therefore calculated some important quantities for several SP in Tables 3 and 4 for the subtraction points in Table 1. The values of the physical quantities which correspond to $SP = 0$ will be taken as the central values.

In Table 3 we give the splitting of the one-loop amplitude ([5]) in the center of the Dalitz plot into a polynomial and a dispersive part, as described in eq. (3.28). Furthermore, we list the first approximation, Φ_{10}, and our final result. Whereas, by construction of the subtraction polynomial, the one-loop amplitude at the center of the Dalitz plot is reproduced for all SP, the relative contributions of the two pieces vary strongly. However, as long as the subtraction points are not too close to the two-pion threshold, the total amplitude given in the last column of Table 3 is rather stable. We therefore consider it most natural to select a small subtraction point. Excluding $SP = 3$, we obtain $A_{\rm tot}(s_0, s_0, s_0) = 1.57 \pm 0.12 + i(0.41 \pm 0.03)$.

Table 4 contains the physical observables for the various subtraction points. The rates in the second last two columns are calculated from eq. (1.9), e.g. with the normalization of the amplitude given by m_1^2. We will discuss the relevance to the

quark masses in the next section.

As may be expected, large subtraction points (near the physical region) yield smaller rates because there the full result is nearer to the one-loop result which is too small. On the other hand, large negative SP do not arbitrarily increase the rates; rather, these remain remarkably stable. Thus it is not possible to (artificially) enhance the rates by playing with the subtraction points. The uncertainty of the subtraction point can be substantially reduced, if the Dalitz plot slopes a, b, c (to be discussed below) could be measured with two percent accuracy; This would allow to narrow down the error bar on Γ to 10 % or 16 eV. At present, the experimental values (which admittedly have larger errors) prefer small SP.

2. Errors in the subtraction constants

Without a next order calculation, the error of the subtraction constants in the polynomial, in particular on γ and δ which vanish at tree level cannot be truly assessed. A reasonable estimate of the errors can be obtained by the following observation by Anisovich and Leutwyler [22]. The current algebra result for the $\eta \to 3\pi$ amplitude has an Adler zero (a value of the kinematic variables where the amplitude vanish), which for finite quark masses is shifted to $s \equiv s_A = \frac{4}{3}m_\pi^2$. This can be easily seen from the tree level result; obviously, the Adler zeroes lie on a straight line. The one-loop amplitude shares this feature (with a slightly shifted s_A), if in addition we fix $s_a = s_c = s_A$ (or $s_a = s_b = s_A$). Moreover, along the line $s_a = s_c$ the slope $\frac{dA}{ds}(s_a = s_c = s_A)$ is practically unchanged compared to the leading order expression $\frac{3}{m_\eta^2 - m_\pi^2}$. This suggests that the amplitude along the line $s_a = s_c$ near s_A is remarkably stable against corrections and that this kinematical point is well suited as subtraction point. One may therefore expect that higher order corrections lie within the usual 25 % range of chiral corrections. Note that it is crucial to stay on the line $s_a = s_c$. For if we consider for example the subtraction polynomial in the form corresponding to an expansion around the point $s_a = 0$, $s_b = s_c$,

$$P = \alpha + \beta s_a + \gamma s_a^2 + \delta(s_b - s_c)^2, \tag{5.2}$$

The coefficients α, β in (5.2) are indeed very different from the current algebra expressions $\alpha^{\mathrm{CA}} = -4m_\pi^2/(m_\eta^2 - m_\pi^2)$, $\beta^{\mathrm{CA}} = 3/(m_\eta^2 - m_\pi^2)$. The amplitude is not stable against corrections along the line $s_b = s_c$ and it is difficult to assign an error bar to α, ...δ in (5.2) as noted before.

We therefore expand around $s_a = s_c = s_A$, i.e.

$$P = \bar{b}z + \bar{c}z^2 + \bar{d}w + \bar{e}w^2 + \bar{f}wz, \tag{5.3}$$

where

$$z = 3s_0 - 2s_A - s_b, \qquad w = s_a - s_c. \tag{5.4}$$

By Bose symmetry, only three of the five constants in (5.3) are independent; for

instance

$$\begin{aligned} \bar{e} &= \frac{\bar{b}-\bar{d}}{6(s_0-s_A)}+\bar{c} \\ \bar{f} &= \frac{\bar{b}-\bar{d}}{2(s_0-s_A)}+2\bar{c} \end{aligned} \tag{5.5}$$

Numerically we find

$$\begin{aligned} \bar{b} &= 4.87\text{GeV}^{-2} \\ \bar{c} &= 13.65\text{GeV}^{-4} \\ \bar{d} &= 11.88\text{GeV}^{-2}. \end{aligned} \tag{5.6}$$

Here, only those contributions from the subtraction polynomial which come from $\bar{A}^{\text{rem}}$ (see section 3.2) have been included. The remainder $R(s_a, s_b, s_c)$ serves only to bring the one-loop amplitude into the form of a dispersion relation and is cancelled once the first iteration step has been performed. As discussed above, the constants s_A and $\bar{b}$ are rather stable agains correctionsknown with very good accuracy. However, $\bar{c}$ receives contributions only at one-loop order and $\bar{d}$ is very sensitive to corrections. For the error estimate, we therefore assume that s_A and $\bar{b}$ are given exactly by (5.6) whereas $\bar{c}$ and $\bar{d}$ are assigned a relative error of 25 %, typical of higher loop-corrections:

$$\begin{aligned} \delta\bar{c} &= 3.41\text{GeV}^{-4} \\ \delta\bar{d} &= 2.97\text{GeV}^{-2}. \end{aligned} \tag{5.7}$$

These errors induce sizeable uncertainties of the constants α, ..., δ in the expansion (5.2) for P (again, the contributions of the remainder $R(s_a, s_b, s_c)$ are not written):

$$\begin{aligned} \alpha &= -1.02 \pm 0.01 \mp 0.34 \\ \beta &= (20.35 \mp 0.72 \pm 5.69)\text{GeV}^{-2} \\ \gamma &= (-1.38 \pm 13.65 \mp 23.72)\text{GeV}^{-4} \\ \delta &= (6.22 \pm 0.0 \pm 2.63)\text{GeV}^{-2}. \end{aligned} \tag{5.8}$$

The first and second errors come from the uncertainty in $\bar{c}$ and $\bar{d}$ respectively. The latter are particularly large, however they are correlated and cancel completely for the polynomial (5.2) evaluated at the center of the Dalitz plot.

The induced error bar on the amplitude at $s_a = s_c = s_0$ can be estimated by calculating the change in $P(s_0, s_0, s_0)$. Only $\delta\bar{c}$ matters of course and we find

$$\delta\bar{A}(s_0, s_0, s_0) \approx \delta P(s_0, s_0, s_0) = \delta\bar{c}(s_a - s_A)^2 = 0.12. \tag{5.9}$$

This is 8 % of the full amplitude corresponding to a 16 % error on the rate, i.e. 26 eV if $Q = Q_{\text{Dashen}}$ is employed. The actual change of the full amplitude is somewhat larger and summarized in Table 7.

The rate is thus very sensitive to the value of the constant $\bar{c}$. If its higher order contributions turned out to be large and positive, using its one-loop value would seriously underestimate the rate. We therefore attempt a more quantitative estimate of the higher order corrections to $\bar{c}$ by considering a twice subtracted dispersion relation, following again Anisovich and Leutwyler [22]. We start by decomposing the amplitude into its isospin components, i.e.

$$\begin{aligned} F(s_a,s_b,s_c) &= M_0(s_a)+(s_a-s_c)M_1(s_b)+(s_a-s_b)M_1(s_c) \\ &\quad +M_2(s_b)+M_2(s_c)-\frac{2}{3}M_2(s_a). \end{aligned} \tag{5.10}$$

This decomposition is ambiguous for unitarity determines only the singular part of the amplitudes M_0, M_1 and M_2. A polynomial in s_a can always be shifted between the isospin amplitudes, a feature which can be used to make the $I=1,2$ parts in F small in the physical region. Then, a dispersive analysis is performed for the function M_0 only, which must satisfy the twice subtracted relation

$$M_0(s_a)=\frac{1}{D(s_a)}\left\{\alpha_0+\beta_0(s_a-s_A)+\frac{(s_a-s_A)^2}{\pi}\int\frac{ds'D(s')f_0^0(s')\frac{2}{3}\bar{M}_0(s')}{(s'-s_A)^2(s'-s_a-i\epsilon)}\right\}, \tag{5.11}$$

if we neglect the small pieces proportional to M_1, M_2 under the integral. The two subtraction constants α_0, β_0 are fixed by the requirement

$$\begin{aligned} M_0(s_A) &= M_0^{1-\text{loop}} \\ \frac{d}{ds_a}M_0(s_A) &= \frac{d}{ds_a}M_0^{1-\text{loop}}(s_A). \end{aligned} \tag{5.12}$$

The 1-loop amplitude enters here only to fix the subtraction constants at the Adler point. As mentioned, the corrections at this point are very small so that this procedure is reasonable. There is however a further implicit assumption in the method, namely the choice of the $I=1,2$ amplitudes. Although it affects the total amplitude, say at the center of the Dalitz plot, rather substantially, the resulting uncertainty on $\bar{c}$ is not important. The contribution to $\bar{c}$ can then be written as a integral over the discontinuity in the s_a channel:

$$\bar{c}^{(M_0)}=\frac{1}{4\pi D(s_A)}\int\frac{ds'D(s')f_0^0(s')[\alpha_0+\beta_0(s'-s_A)+\frac{2}{3}\bar{M}_0(s')]}{(s'-s_A)^3}. \tag{5.13}$$

Solving eq. (5.11) by iteration we obtain $\bar{c}^{(M_0)}=(7.9+i0.5)\text{GeV}^{-4}$, which has to be compared to the contribution of $M_0^{1-\text{loop}}$, $c^{(M_0,1-\text{loop})}=5.85\text{GeV}^{-4}$. Thus

$$\delta\bar{c}=2.05\text{GeV}^{-4} \tag{5.14}$$

which lies perfectly well within the range established above. However, the sign of the correction (positive) is now well understood. The reason is that current

algebra underestimates the $I = 0$ s-wave rescattering, hence yielding too small a discontinuity.

We conclude that the actual value of $\delta\bar{c}$ is higher than the one-loop value; and we will adopt $\bar{c}^{(M_0)} = (7.9 + i0.5)\text{GeV}^{-4}$ as the most likely number. It shifts the amplitude at the center to $1.71 + i0.45$ (of which 1.47 is in the subtraction polynomial) or by about 9 % [9].

3. Asymptotic behaviour of the $\pi\pi$-phase shift

In sect. 3 we mentioned an ambiguity to the solution of Khuri-Treiman equations due to the so far unspecified asymptotic behaviour of the $\pi\pi$-phase shifts. Here we give a quantitative estimate of the effect on our results. We neglect the $I = 1, 2$ phase shifts and consider the approximate solution $F = P + \Phi_{10}$, where Φ_{10} is given explicitly in eq. (4.21). This approximation is actually very close to our final numerical solution, c.f. Table 3. Now we study two cases with distinct asymptotic behaviour of both, phase shift and amplitude: i) $\delta_0^0(s) \to 0$ and $Q = 0$, i.e. $F(s) \sim s^2$ and ii) $\delta_0^0(s) \to \pi$ and $Q = \text{const.} \neq 0$, where we fine tune Q such that the amplitude has the improved asymptotic behaviour $F \sim s$. In the first case we use the phase shift as employed before, given in eq. (B.2) and denoted here by $\delta_0^{0,\,\text{Schenk}}(s)$. In case ii) we need a model which guides the phase to its asymptotic value π. We take

$$\delta_0^0(s) = \begin{cases} \delta_0^{0,\,\text{Schenk}}(s), & s \leq s_{00} \\ \delta_0^{0,\,\text{Schenk}}(s) \left(\frac{s}{s_{00}}\right)^h, & s_{00} \leq s \leq \Lambda_h^2 \\ \pi, & s > \Lambda_h^2, \end{cases}$$

with $s_{00} = (865\text{MeV})^2$ and Λ_h^2 is the scale where the phase reaches its asymptotic value. We consider two choices $h = 1/4$ and $1/8$ with corresponding scales $\Lambda_{1/4}^2 = (2.16\text{GeV})^2$ and $\Lambda_{1/8}^2 = (4.87\text{GeV})^2$ respectively.

We then calculate the difference $\delta F = F^{(i)} - F^{(ii)}$ at the center of the physical region for various subtraction points SP. The maximal difference we obtain is $\delta F = 0.015 - i*0.020$, or 1 % and 5 % of the full amplitude for real and imaginary part respectively. This in turn implies an error on the rate $\bar{\Gamma}$ of less than 3 % or $\approx$ 4eV. The exercise shows that rather different assumptions on the asymptotic behaviour imply only modest changes of the amplitude in the low energy region. Here, taking three subtractions pays visibly. The same estimate for a twice subtracted relation (see below) yields an uncertainty in the real part of the amplitude of already $\approx 5\%$ or $\approx$ 17eV on the rate.

4. Technical uncertainties

We conclude with some remarks on the structure and convergence of our iteration. As described in section 4, we distinguish two iterations, namely the iteration when solving the dispersion relation (m-iteration, in the $I = 0$ rescatterings) and the one in powers of the weaker $I = 2, 1$ rescatterings (k-iteration). We will discuss some

[9] We have taken the subtraction point $SP = 0$.

exemplary numerical results and comment on the general trends. We will always use the subtraction at zero with the corresponding values of the polynomial.

To illustrate the m-iteration, we take the succesive values of the contribution to pure $I = 0$ problem as considered by Neveu and Scherk. Writing the amplitude U in the form (see eq. (4.18))

$$U_k(s) = \sum_1^\infty \Phi_{mk}(s) \tag{5.15}$$

we find in the center of the Dalitz plot the following numbers:

$$\mathrm{Re}\Phi_{10} = 0.1828 \quad \mathrm{Re}\Phi_{20} = -0.0631 \quad \mathrm{Re}\Phi_{30} = 0.0051 \quad \mathrm{Re}\Phi_{40} = 0.0001 \tag{5.16}$$

This suggests that the iteration in the $I = 0$ scattering phase converges nearly like a geometrical series with a coefficent of 0.3. We have found this behaviour over the whole Dalitz plot and for all values of k. The iteration is therefore terminated at $m = 5$.

Next we consider the k-iteration. As example, we take again the amplitudes U, V, W at the center. We obtain:

$U_0 = 0.1248 + i0.4786$ no $I = 1, 2$ corrections
$U_1 = -0.0180 + i0.0638$ one $I = 1, 2$ iteration
$U = 0.1145 + i0.5431$ total result
$V_1 = 0.0407 - i0.0617$ one $I = 1, 2$ corrections
$V = 0.0343 - i0.0649$ total
$W_1 = -0.0038 - i0.0003$ one $I = 1, 2$ corrections
$W = -0.0039 + i0.0002$ total $I = 1, 2$ iteration

Again, the convergence of the results is rather good; consecutive terms decrease by about 10 to 15 percent.

To appreciate the degree to which the final result fulfills unitarity, we take amplitude at the center of the Dalitz plot for various stages of the iteration. Including only the first iteration, Φ_{10}, the value of the amplitude is $A_{app} = 1.57 + i0.5017$. Unitarity is checked by inserting this (and the corresponding values for all s) value into the dispersion relation for the total amplitude which yields a new value, say A'_{app} on the left hand side and calculate the relative difference $d = (A_{app} - A'_{app})/|A'_{app}|$. At the center of the Dalitz plot, we obtain for this deviation $0.0441 - i0.0301$ which indicates that unitarity is fulfilled to about six percent. Taking now the full amplitude, $1.57 + i0.4128$. The unitarity check now yields only $d = 0.0007 + i0.0002$. The iteration has improved the unitarity drastically, although the central value of the amplitude is not much changed.

Another result of interest is the quality of the Neveu-Scherk Φ_{10} iteration and the relative sizes of the various isospin amplitudes U, V and W. The sum $P + \Phi_{10}$ corresponds rather accurately to the final value. This is accidental. If we just solve the complete Neveu-Scherk problem, e.g. only include $I = 0$ rescatterings, the result would be $U = 0.1248 + i0.4786$ and Φ_{10} would not be a good approximation. On the other hand, the complete calculation yields $U = 0.1145 + i0.5431$, $V = 0.0343 -$

$i0.0065$, $W = -0.0039 + i0.0002$. This shows that the contribution from V is quite substantial, and that U alone does not saturate the amplitude at all. Nevertheless we note that $|V/U|$ is roughly about a third, which justifies our perturbative treatment of V (and W).

A further error comes from the arbitrary cutoff of the dispersion integral. Changing it from $82m_\pi^2$ to $164m_\pi^2$, the rates vary at most by 1 eV and thus the variation is negligible.

Also, the low energy constant L_3 [2] is not very precisely known. Varying it within the error bars yields the small ranges

$\Gamma_{\eta\to\pi^+\pi^-\pi^0} : 182.1 - 181.1eV$
$\Gamma_{\eta\to\pi^0\pi^0\pi^0} : 250.9 - 253.5eV$
$a : -1.21 - -1.12$
$b : 0.25 - 0.23$
$c : 0.10 - 0.09$
for the one-loop value of the constant $\bar{c}$.

Apart from the changes in a, these variations are small. A more precise measurement of a could therefore restrict L_3.

5.2 Rates and Dalitz Plot Distribution

Let us turn now to the values of the physical quantities. If we take the one-loop value for the constant $\bar{c}$, the rate for $\eta \to \pi^+\pi^-\pi^0$, normalized by m_1^2, is

$$\Gamma = (180 \pm 40) \text{ eV}. \tag{5.17}$$

The error given reflects our estimate of the uncertainty of 25 % of $\bar{c}$. On the other hand, if the improved value for $\bar{c}$ is used, the rate becomes

$$\Gamma = 209 \text{ eV}. \tag{5.18}$$

We estimate the remaining error on this result to be about 20 eV. Since the one-loop value of $\bar{c}$ is most certainly too small, the result in eq. (5.18) should be more reliable than the value in eq. (5.17) The corresponding values for the decay into neutral pions are (252 ± 56)eV and 295eV. Thus, the rates are not substantially larger than the previous results, if the the one-loop value of $\bar{c}$ is taken. However, if its improved value is employed by taking into account the rescatterings through the Khuri-Treiman equations, the corrections are substantial, although the result is still considerably below the experimental one. The size of the corrections are qualitatively reasonable: since the one-loop corrections amount to about 50 % in amplitude, next order corrections might be expected at about 40 eV, roughly the value we found.

The ratio

$$r = \frac{\Gamma_{\eta\to\pi^0\pi^0\pi^0}}{\Gamma_{\eta\to\pi^+\pi^-\pi^0}} \tag{5.19}$$

between the rates of the neutral and charged pion channel takes the values

$$r = 1.40 \pm 0.03 \tag{5.20}$$

and

$$r = 1.41 \pm 0.03 \tag{5.21}$$

for the two values of $\bar{c}$, respectively. The values correspond to the the small subtraction points SP considered; the error is obtained by varying the SP between -10 and 2 (see Table 4). In comparison, the value $r = 1.43$ was obtained in Ref. [5]. The particle data group quotes

$$\begin{aligned} r &= 1.35 \pm 0.05 \qquad \text{"our fit"} \\ r &= 1.27 \pm 0.14 \qquad \text{"our average"}, \end{aligned} \tag{5.22}$$

favoring smaller values for r, in particular almost excluding the current algebra result. Recently, r has been remeasured in a direct measurement [37]

$$r = 1.44 \pm 0.09 \pm 0.01 \tag{5.23}$$

with smaller errors than previously and which is in very good agreement with our result and the one-loop value but somewhat below the current algebra prediction of $r = 1.51$.

The distribution over the Dalitz plot is conventionally described by the two variables x and y

$$x = \frac{\sqrt{3}}{2m_\eta Q_\eta}(s_c - s_b) \tag{5.24}$$

$$y = \frac{3}{2m_\eta Q_\eta}((m_\eta - m_\pi)^2 - s_a) - 1 \tag{5.25}$$

$$Q_\eta = m_\eta - 2m_{\pi^+} - m_{\pi^0}. \tag{5.26}$$

Since Q_η is small, it is important to keep the masses of the charged and neutral pions different. The mass difference is generated by electromagnetic corrections. However, as discussed in the first section, the other electromagnetic contributions to the decay amplitude are small and can be neglected.

The Dalitz plot distribution $|A(x,y)|^2$ can be parametrized by a second order polynomial. For the decay into charged and neutral pions we may write, respectively,

$$\begin{aligned} |A^{+-0}(x,y)|^2 &= N^{+-0}\left(1 + ay + by^2 + cx^2\right), \\ |A^{000}(x,y)|^2 &= N^{000}\left(1 + g(x^2 + y^2)\right). \end{aligned} \tag{5.27}$$

Of course, the neutral pion mass must be used for x and y in the second expression.

The various determinations of the slopes a, b, c and g are as follows:

Gasser and Leutwyler [5]: $a = -1.33, b = 0.42, c = 0.08$

Layter et al. (exp)[38]: $a = -1.08 \pm 0.014, b = 0.034 \pm 0.027, c = 0.046 \pm 0.031$
Gormley et al. (exp)[39]: $a = -1.17 \pm 0.02, b = 0.21 \pm 0.03, c = 0.06 \pm 0.04$
Amsler et al. (exp)[37]: $a = -0.94 \pm 0.15, b = 0.11 \pm 0.27$
Alde et al. (exp)[40]: $g = -0.044 \pm 0.046$
This work: $a = -1.16, b = 0.24, c = 0.09, g = -0.028$ (one-loop value for $\bar{c}$)
$a = -1.16, b = 0.26, c = 0.10, g = -0.014$ (improved value for $\bar{c}$).

We see that our numbers are very near to the experimental values, in fact closer than the one-loop results. The values of a for negative SP are somewhat too large, while the result for $SP = 0$ correspond nicely to the result of Gormley et.al. Unfortunately, the two most accurate experiments are mutually inconsistent and thus preclude a definite statement; measuring the slopes with larger accuracy would remove the uncertainties inherent in the choice of the subtraction points. The quadratic slope parameter of the neutral decay mode, g, is experimentally compatible with zero. We observe that the slopes (with the exception of g) do not depend strongly on the value of $\bar{c}$.

However, the shape of the amplitude changes when compared to the one-loop amplitude. In Fig. 3 we plot the real part of our numerical solution (with the one-loop value of $\bar{c}$) along the line $s_a = s_c$, together with the current algebra prediction as well as the chiral perturbation theory one-loop amplitude. At small s, all amplitudes are close together which reflects the fact that we have subtracted at $s_a = 0$. The cusp generated by the two-pion threshold is more pronounced in the solution taking into account the corresponding final state interactions to all orders. However, the requirement of unitarity bends the amplitude down more strongly in the physical region, leading to a value of the amplitude at the center of the Dalitz plot close to the value obtained by one-loop ChPT. At the same time, the slope of the amplitude is reduced substantially giving a smaller values of the linear slope parameter of the Dalitz plot distribution. The imaginary part is seen to be enhanced over the whole physical region, c.f. Fig. 4. This was to be expected, as the one-loop amplitude gives only the leading term to the imaginary part. The figures for the improved $\bar{c}$ have a similar shape, but with different normalization corresponding to the larger rate discussed above.

5.3 Two Subtractions

We turn briefly to the twice subtracted dispersion relation. Starting from the current algebra polynomial, we obtain the results in Table 6, taking the subtraction points in Table 5. We have used the same scattering phase as in the three times subtracted case, and set the polynomial Q equal to zero. This time, the rates grow fast if we change the subtraction points to large negative values. On the other hand, this increase is accompagnied by an unreasonable change of the slopes a and b as well as unacceptable values of r. We expect similar changes, if we vary the asymptotic behaviour of the amplitude and the phase (see above). We conclude that artificially enhancing the rates with large negative subtraction points does not yield correct

results and that the higher order terms in the subtraction polynomial are essential. An alternative approach would be to use the one-loop subtraction data, but to maintain a twice subtracted relation. We expect in this case larger uncertainties from the assumption of elastic unitarity as well as from the asymptotic ambiguities.

Roiesnel and Truong [32] were the first to invoke unitary corrections to enhance the decay rate. These authors obtained satisfactory values for the rates, using a once subtracted dispersion relation; Their analysis was restricted to $I = 0$ rescatterings, but only for one part of the amplitude. As a result, their discontinuity is not given by the usual form, but is larger by a factor 9/5. Since the sign of the $I = 2$ contribution is negative, this factor in fact gets enhanced because the $I = 0, 2$ pieces suffer an artificial cancellation. If this factor is omitted, the result is not as dramatic and close to our results for $SP = 0$. As noted, the dispersion relation with one subtraction is subject to large ambiguities and thus the result will be beset with high uncertainties.

6 Conclusions

The decay amplitude of $\eta \to 3\pi$ is proportional to the quark mass difference $(m_d - m_u)$ and thus provides one of the ingredients to determine the important ratio $\frac{m_u}{m_d}$. Including also higher orders in chiral perturbation theory, the decay rate can indeed be written as

$$\Gamma = (Q_{DT}/Q)^4 \bar{\Gamma} \tag{6.1}$$

where

$$Q^{-2} \equiv \frac{m_d - m_u}{m_s - \hat{m}} \cdot \frac{m_d + m_u}{m_s + \hat{m}} \tag{6.2}$$

with $\hat{m} \equiv \frac{1}{2}(m_d + m_u)$. Q_{DT} is the value of Q if Dashen's theorem for the electromagnetic kaon mass difference is used (see eq. (1.9)) and $\bar{\Gamma}$ the corresponding width as given in the previous chapter.

Using the value Q_{DT} (or the corresponding and long established values for the quark mass ratios), the one-loop ChPT prediction for the rate given by Gasser and Leutwyler [5] has been considerably below the experimental number. Theoretically, the rate can be increased by lowering the ratio m_u/m_d [20] or by including further corrections in $\bar{\Gamma}$. In particular, it has long been suspected that the unitary corrections may be sufficient to enhance the rate sufficiently.

The existing framework embodied in the so called Khuri-Treiman equations [24] allows to take into account rescatterings of two pions which are thought to dominate. Some time ago, Roisnel and Truong [32] claimed that in fact these corrections solve the problem, but as explained in section 5 (see also [5]), we believe that their results are an overestimate.

In this paper we have calculated the unitary corrections using the Khuri-Treiman equations (which include the $I = 0, 2$ pion pion rescatterings), complemented with the $I = 1$ interactions. To specify these dispersion relations completely, that is to define the subtraction method, we have used an iterative procedure for solving it

which accounts in lowest order for the one-loop ChPT results of Gasser and Leutwyler. This forced us to a three times subtracted dispersion relation with rather fast convergence and little dependence on the unknown high energy scattering phase. In this approach, the subtraction polynomial is quadratic in the invariant momenta, rather than the linear form of current algebra. The major source of errors lies in the choice of the subtraction points and, particularly, in the uncertainties in the subtraction constants. The constants connected to the quadratic terms vanish at tree level and only start at the one-loop level; thus their one-loop value is rather uncertain. In section 5 we have described how this problem can be overcome (following recent work of Anisovich and Leutwyler [22]), and have given a reasonable estimate of the constant $\bar{c}$. We have chosen to give the results corresponding to both their one-loop value and to the improved one. Using everywhere the new value of f_π [6], the rate corresponding to the the one-loop value is

$$\bar{\Gamma} = (180 \pm 40)\text{eV}, \tag{6.3}$$

while the improved number of $\bar{c}$ yields

$$\bar{\Gamma} = 209\text{eV} \tag{6.4}$$

and where we estimate the remaining errors to be about $20eV$. We view the second result as the more reliable one. Although the corrections are quite large, they do not suffice to explain the experimental value of (281 ± 28)eV.

From eq. (6.4) we obtain

$$Q = 22.4 \pm 0.9. \tag{6.5}$$

while the rate of 180 eV in (6.3) would imply $Q = 21.6 \pm 1.3$. In contrast, $Q_{DT} = 24.1$.

These lower values of Q can obviously be accounted for if the ratio $\frac{m_u}{m_d}$ is lowered, and another mass ratio, say $\frac{m_d+m_u}{m_s}$ is kept fixed. In this case, $\frac{m_u}{m_d}$ is reduced from 0.57 to 0.49 ± 0.04 or to 0.52 ± 0.03 depending on whether eq. (6.3) or eq. (6.4) is used. Thus, while it may be somewhat smaller than previously thought, the up quark mass does not vanish [10]. We note that the somewhat lower value of $\frac{m_u}{m_d}$ in [20] was obtained with a changed value of $\frac{m_d+m_u}{m_s}$. The constant Q can also be determined from electromagnetic corrections to the meson masses. As already noted in [20], these lower values of Q correspond roughly to the one obtained from the kaon mass difference, if electromagnetic corrections are positive and large as found in [18].

We have also determined the slopes in the Dalitz plot distributions; the results are given in the last section. We find that the ratio r between the rates of the neutral and charged pion mode remains roughly at 1.4 which is also favored experimentally [37]. On the other hand, the slopes change from their one-loop ChPT values; our number for a is higher than the previous result and nearer to the experimental value.

[10] our analysis is based on the assumption of the validity of standard chiral perturbation theory. In contrast, a treatment along the lines of Ref. [14] might lead to different results; however the larger quark masses in that scheme exclude a zero mass automatically

The experimental situation is rather unsatisfactory. The decay rates are normalized with respect to the decay with $\Gamma(\eta \to \gamma\gamma)$, where the results from two-photon production disagree with those from Primakoff production. The two-photon measurements seem more reliable; however, in order to resolve the issue completely a reanalysis of the Primakoff data would be necessary. The Dalitz plot distribution of $\eta \to \pi^+\pi^-\pi^0$ has been measured with rather high accuracy [39, 38]. However, the assumptions made by these authors are not compatible and do not allow comparison ot the numerical values. A recent experiment [37] has still too large error bars in order to be conclusive. As our results show, there is a rather strong correlation between rates and slope parameters and a more acurate measurement of the latter would fix the rates, and thereby the up quark mass better.

Acknowledgments: We benefited much from discussions with J. Bronzan, B. Holstein, J. Gasser, A. Salathe, J. Stern, J. Donoghue and, in particular, H. Leutwyler who shared with us much of his recent results prior to publication. Large part of the work by J.K. was done while at the Department of Physics and Astronomy, University of Massachusetts, Amherst; J.K. and D.W. also thank the Institute for Nuclear Theory in Seattle where some of the work was done for hospitality.

References

[1] S. Weinberg, Physica **A96** (1979), 327. J.F. Donoghue, E. Golowich and B.R. Holstein 'Dynamics of the Standard Model', CUP, Cambridge 1992. H. Leutwyler, Ann. Phys. **235** (1994), 165; H. Leutwyler, 'Principles of Chiral Perturbation Theory' BUTP-94/13 (1994).

[2] J. Gasser and H. Leutwyler, Nucl. Phys. **B250** (1985), 517.

[3] H. Osborn and D. J. Wallace, Nucl. Phys. **B20** (1970), 23; J. A. Cronin, Phys. Rev. **161** (1967), 1483.

[4] Review of Particle Properties, Phys. Rev. **D50** (1994). The value of (281 ± 28) eV corresponds to the average value given for the rate. There are, however, conflicting measurements; excluding the value obtained from the Primakoff effect, the 3π rate would be (310 ± 20) eV.

[5] J. Gasser and H. Leutwyler, Nucl. Phys. **B250** (1985), 539.

[6] B.R. Holstein, Phys. Lett. **244** (1990), 83; Review of Particle Properties, Phys. Rev. **D50** (1994).

[7] J. Gasser and H. Leutwyler, Phys. Rep. **87** (1982), 77; H. Leutwyler, Nucl. Phys. **B337**(1990), 108; J.F. Donoghue and D. Wyler, Phys. Rev. **D45** (1992), 892; D. Wyler, 'Light Quark Masses beyond Leading Order', Proc. XVI Kazimierz Meeting, World Scientific 1994, Edts. Z. Ajduk et. al; H. Leutwyler 'Masses of the Light Quarks' BUTP-94/8 (1994).

[8] R. Peccei, in 'CP Violation', (C. Jarlskog ed.), World Scientific, Singapore 1989.

[9] D. G. Sutherland, Phys. Lett. **23** (1966), 384.

[10] J.S. Bell and D.G. Sutherland, Nucl. Phys. **B4** (1968), 315

[11] P. Dittner, P.H. Dondi and S. Eliezer, Phys. Rev. **D8** (1973), 2253.

[12] R. Baur, J. Kambor and D. Wyler, in preparation.

[13] J. Gasser and H. Leutwyler, Nucl. Phys. **B250** (1985), 465.

[14] J. Stern, H. Sazdjian and N.H. Fuchs, Phys. Rev. **D47** (1993), 3814; M. Knecht and J. Stern, "generalized Chiral Perturbation Theory", preprint IPNO/TH 94-53, to appear in the second edition of the DaΦne Physics Handbook, L. Maiani, G. Pancheri and N. Paver Eds., INFN, Frascati

[15] D. Kaplan and A. Manohar, Phys. Rev. Lett. **56** (1986), 1994.

[16] See Ref. [7], in particular the paper by Leutwyler (1994).

[17] R. Dashen, Phys. Rev. **183** (1969), 1245.

[18] J.F. Donoghue, B.R. Holstein, and D. Wyler, Phys. Rev. **D47** (1993), 2089; J. Bijnens, Phys. Lett. **B306** (1993), 343.

[19] R. Urech, Nucl. Phys. **B433** (1995), 234.

[20] J.F. Donoghue, B.R. Holstein and D. Wyler, Phys. Rev. Lett. **69** (1992), 3444.

[21] A. Pich, in "Rare decays of Light Mesons", Ed. B.Mayer, Editions Frontieres, 1990.

[22] A. V. Anisovich and H. Leutwyler, Bern University preprint BUTP 95/1; H. Leutwyler, private communication.

[23] G. Ecker et. al., Nucl. Phys. **B321** (1989), 311.

[24] N. N. Khuri and S. B. Treiman, Phys. Rev. **119** (1960), 1115.

[25] V. V. Anisovich, A. A. Ansel'm, and V. N. Gribov, JETP **15** (1962), 159.

[26] G. Bonnevay, Nuov. Cim. **30** (1963), 1325.

[27] J. Bronzan and C. Kacser, Phys. Rev. **132** (1963), 2703.

[28] C. Kacser, Phys. Rev. **132** (1963), 2712.

[29] J. Bronzan, Phys. Rev. **134** (1964), B687.

[30] I. J. R. Aitchison, Phys. Rev. **133** (1964), B1257; I. J. R. Aitchison, Phys. Rev. **137** (1965), B1070; R. Pasquier and J. Y. Pasquier, Phys. Rev. **170** (1968), 1294.

[31] A. Neveu and J. Scherk, Ann. Phys. **57**, 39 (1970).

[32] C. Roiesnel and T.N. Truong, Nucl. Phys. **B187**, 293 (1981).

[33] A.V. Anisovich, St. Petersburg preprint TH-62-1993, to be published in "Physics of Atomic Nuclei", **58** (1995).

[34] J. Gasser and H. Leutwyler, Ann. Phys. **158** (1984), 142.

[35] C. Riggenbach et al, Phys. Rev. **D43** (1991), 127.

[36] D. Jackson, in 'Dispersion Relations', (G. R. Screaton ed), Oliver and Boyd, London, 1961.

[37] Crystal Ball collaboration, C. Amsler et al. Phys. Lett. **B346** (1995), 203.

[38] J.G. Layter et al., Phys. Rev. **D7** (1973), 2565.

[39] M. Gormley et al., Phys. Rev. **D2** (1970), 501.

[40] D. Alde et al., Zeitsch. Phys. **C25** (1984), 225.

[41] A. Schenk, Nucl. Phys. **B365** (1991), 97.

[42] J. Gasser and H. Leutwyler, Phys. Lett. **B125** (1983), 325.

Appendix A

In this Appendix we give the three projections of the subtraction polynomial P. Since P has no cuts, the integrals as defined in section 2 are trivial and may be performed explicitly.

The second order subtraction polynomial is of the form

$$P(s_a, s_b, s_c) = \alpha + \beta s_a + \gamma s_a^2 + \delta(s_b - s_c)^2 \tag{A.1}$$

and we need the projections $\overline{s_b^n}$ for $n = 0, .., 3$. The corresponding results are

$$\begin{aligned}
\overline{1} &= 1 \\
\overline{s_b} &= \frac{3s_0 - s_a}{2} \\
\overline{s_b^2} &= \left(\frac{3s_0 - s_a}{2}\right)^2 + \frac{K^2(s_a)}{3} \\
\overline{s_b^3} &= \frac{3s_0 - s_a}{2} \cdot \left[\left(\frac{3s_0 - s_a}{2}\right)^2 + K^2(s_a)\right].
\end{aligned} \tag{A.2}$$

We now insert P into eq. (2.26), reexpress $s_c = 3s_0 - s_a - s_b$ and obtain

$$\begin{aligned}
\overline{P}(s_a) &= \alpha + \beta s_a + \gamma s_a^2 \\
&+ \delta(4\overline{s_b^2} - 4\overline{s_b}(3s_0 - s_a) + (3s_0 - s_a)^2) \\
&= \alpha + \beta s_a + \gamma s_a^2 + \delta\frac{4K^2(s_a)}{3}.
\end{aligned} \tag{A.3}$$

For $\tilde{P}(s_a)$ we get from eq. (2.27)

$$\begin{aligned}
\tilde{P}(s_a) &= \alpha + \beta\overline{s_b} + \gamma\overline{s_b^2} \\
&+ \delta(\overline{s_b^2} - 2\overline{s_b}(3s_0 - 2s_a) + (3s_0 - 2s_a)^2) \\
&= \alpha + \beta\frac{3s_0 - s_a}{2} - \delta s_a(3s_0 - 2s_a) \\
&+ (\gamma + \delta)\left[\left(\frac{3s_0 - s_a}{2}\right)^2 + \frac{K^2(s_a)}{3}\right].
\end{aligned} \tag{A.4}$$

Turning finally to $\hat{P}$ its insertion into eq. (2.36) yields

$$\begin{aligned}\hat{P}(s_a) &= -\frac{3}{4K^2(s_a)}[\,2\{\alpha\overline{s_b}+\beta\overline{s_b^2}+\gamma\overline{s_b^3}\\ &+ \delta(\overline{s_b^3}-2\overline{s_b^2}(3s_0-2s_a)+\overline{s_b}(3s_0-2s_a)^2\}\\ &\quad -(3s_0-s_a)\{\alpha+\beta\overline{s_b}+\gamma\overline{s_b^2}\\ &+ \delta(\overline{s_b^2}-2\overline{s_b}(3s_0-2s_a)+(3s_0-2s_a)^2)\}]\\ &= -\frac{1}{2}\left[\beta+(\gamma-\delta)(3s_0-s_a)\right].\end{aligned} \tag{A.5}$$

Appendix B

In this Appendix we discuss the parametrization of the different pion-pion phase shifts used in our numerical computations and disply the resulting Omnès function.

A careful analysis of the different restrictions on the phase shifts is carried out in Ref. [41]. There are two main points to be respected, namely first the threshold behaviour of $\mathrm{Re}f_l^I$

$$\mathrm{Re}f_l^I(s) = (\frac{s-4}{4})^l\left(a_l^I + b_l^I(\frac{s-4}{4}) + ...\right) \tag{B.1}$$

where we used the notations of section 2 and where a_l^I denote the different scattering lengths, b_l^I the corresponding slope parameters. Second, one has to implement that the phase shifts pass through $\frac{\pi}{2}$ at some experimentally known values $s = s_l^I$ of the energy. A simple parametrization respecting those conditions is given by [41]

$$\begin{aligned}\tan\delta_l^I(s) = \sqrt{\frac{s-4}{s}}\cdot(\frac{s-4}{4})^l\cdot\frac{s_l^I-4}{s_l^I-s}\\ \cdot\left(a_l^I+\tilde{b}_l^I(\frac{s-4}{4})+c_l^I(\frac{s-4}{4})^2\right)\end{aligned} \tag{B.2}$$

where the threshold expansion is reproduced with

$$\tilde{b}_l^I = b_l^I - a_l^I\frac{4}{s_l^I-4} + (a_l^I)^3\delta_{l0}. \tag{B.3}$$

As the experimental data on pion-pion scattering near threshold are rather poor one uses the results of ChPT for the scattering length [13, 42]

$$\begin{aligned}&a_0^0 = 0.20, \quad a_0^2 = -0.042, \quad a_1^1 = 0.037,\\ &b_0^0 = 0.24, \quad b_0^2 = -0.075.\end{aligned} \tag{B.4}$$

The remaining data are extracted from experiment

$$\begin{aligned}&b_1^1 = 0.005,\\ &c_0^0 = 0, \quad c_0^2 = 0, \quad c_1^1 = 0,\\ &s_0^0 = 38.45, \quad s_0^2 = -24.11, \quad s_1^1 = 30.39\end{aligned} \tag{B.5}$$

where s_l^I is given in units of m_π^2 as usual. These values correpond to the 'best fits' in [41]. We remark that the constraints of the Roy equation around $s = 4$ are taken into account in this parametrization.

We already noted that all the numerical integrals will be cut off. In order to avoid discontinuities in the numerical integrations, caused by the step-function induced from the cut-off, we bring the phases smoothly down to zero multiplying them with the exponential suppression factor

$$e^{-k\cdot(s-s_0^0)^4} \tag{B.6}$$

ensuring differentiability at s_0^0. For k we chose the value $k = 10^{-5}$.

We do not give explicitely the numerical result for the Omnès function. We just note that instead of working directly with the definition in eq. (4.10) we prefer to go over to the once subtracted form

$$D(z) = e^{-\frac{z}{\pi}\int_4^\infty ds' \frac{\delta_0^0(s')}{s'(s'-z)}}. \tag{B.7}$$

This is possible as we are dealing only with fractions of such functions in which the extra contribution from the subtraction point at $z = 0$ cancels. The advantage of subtracting here is the better numerical convergence of the integrals.

Appendix C

In this Appendix we analyse possible consequences of the singularities occuring in the projected amplitudes as displayed in eqs. (2.44) and (2.45). We show in particular that for physical values of the energy, $s + i\varepsilon$, the amplitude resulting from the dispersion integrals is finite.

Within the iterative procedure we have to perform dispersion integrals over projected functions having poles at $s = (m-1)^2$ to obtain certain contributions to the amplitudes in question. As long as the value of the external variable s is not around $s = (m-1)^2$ there are no problems with the integrations. We have thus to analyse only the case $s \sim (m-1)^2$ where the two types of integrals are of the form

$$\text{const.} \cdot \int_{(m-1)^2-\delta-g}^{(m-1)^2-\delta+g} ds' \frac{1}{s' - (m-1)^2 + \delta - i\varepsilon} \cdot \frac{1}{((m-1)^2 - s')^{\frac{1}{2}+n}} + \text{finite}. \tag{C.1}$$

Above we introduced the two positive constants $g > \delta > 0$ dealing thus with the case $s = (m-1)^2 - \delta \to (m-1)^2$ from below. The other case is then treated similarly. g should be small in the sense that we may replace the full integrand by its above reduction to the two rational functions. 'finite' denotes the obviously finite rest and n the two cases coming from eq. (2.44) with $n = 0$ and from eq. (2.45 with $n = 1$. After a change of variable $s' \to x \equiv s' - (m-1)^2 + \delta$ we obtain

$$I_n \equiv \int_{-g}^{+g} dx \frac{1}{x - i\varepsilon} \cdot \frac{1}{(-x+\delta)^{\frac{1}{2}+n}} \tag{C.2}$$

discarding all unimportant contributions to eq. (C.1). Using the Sokhotsky-Plemelj formula we obtain the principal value integral

$$I_n = i\pi \frac{1}{\delta^{\frac{1}{2}+n}} + P\int_{-g}^{+g} dx \frac{1}{x} \cdot \frac{1}{(-x+\delta)^{\frac{1}{2}+n}}. \tag{C.3}$$

As the square-root has a cut we have to distinguish the cases $-x+\delta > 0$ and $-x+\delta < 0$.

For $-x+\delta > 0$ we obtain

$$\int dx \frac{1}{x} \cdot \frac{1}{(-x+\delta)^{\frac{1}{2}+n}} = \frac{2}{\delta^{\frac{1}{2}+n}} \int dz \frac{1}{z^2-1} \cdot \frac{1}{z^{2n}} \tag{C.4}$$

making the substitution $z \equiv \sqrt{\frac{-x+\delta}{\delta}}$. For $n=0$ this leads to the contribution

$$-\frac{1}{\delta^{\frac{1}{2}}} \log \frac{\sqrt{\frac{g+\delta}{\delta}}-1}{\sqrt{\frac{g+\delta}{\delta}}+1}, \tag{C.5}$$

for $n=1$ to

$$-\frac{1}{\delta^{\frac{3}{2}}} \left\{ 2 \cdot \sqrt{\frac{\delta}{g+\delta}} + \log \frac{\sqrt{\frac{g+\delta}{\delta}}-1}{\sqrt{\frac{g+\delta}{\delta}}+1} - 2 \cdot \lim_{x\to\delta} \sqrt{\frac{\delta}{-x+\delta}} \right\} \tag{C.6}$$

where we properly distinguished the two cases $|z|<1$ and $|z|>1$ in the range of integration and where the principal value prescription leads to the cancelation of the infinities at $x=0$.

For $-x+\delta < 0$ we have to continue analytically. With $\sqrt{-x+\delta} \equiv i\sqrt{x-\delta}$ we find

$$\int dx \frac{1}{x} \cdot \frac{1}{(-x+\delta)^{\frac{1}{2}+n}} = (-)^n \frac{-2i}{\delta^{\frac{1}{2}+n}} \int dz \frac{1}{z^2+1} \cdot \frac{1}{z^{2n}} \tag{C.7}$$

making the substitution $z \equiv \sqrt{\frac{x-\delta}{\delta}}$. For $n=0$ this leads to the contribution

$$-\frac{2i}{\delta^{\frac{1}{2}}} \arctan \sqrt{\frac{g-\delta}{\delta}}, \tag{C.8}$$

for $n=1$ to

$$-\frac{2i}{\delta^{\frac{3}{2}}} \left\{ \sqrt{\frac{\delta}{g-\delta}} + \arctan \sqrt{\frac{g-\delta}{\delta}} - \lim_{x\to\delta} \sqrt{\frac{\delta}{x-\delta}} \right\}. \tag{C.9}$$

Here no further distinctions have to be made.

We collect all the contributions for $n=0$

$$I_0 = \frac{1}{\delta^{\frac{1}{2}}} \left\{ i\pi - \log \frac{\sqrt{\frac{g+\delta}{\delta}}-1}{\sqrt{\frac{g+\delta}{\delta}}+1} - 2i \arctan \sqrt{\frac{g-\delta}{\delta}} \right\} \tag{C.10}$$

and for $n = 1$

$$I_1 = \frac{1}{\delta^{\frac{3}{2}}}\{i\pi - 2\cdot\sqrt{\frac{\delta}{g+\delta}} - \log\frac{\sqrt{\frac{g+\delta}{\delta}}-1}{\sqrt{\frac{g+\delta}{\delta}}+1} - 2i\sqrt{\frac{\delta}{g-\delta}} \tag{C.11}$$
$$-2i\arctan\sqrt{\frac{g-\delta}{\delta}} + 2\cdot\lim_{x\to\delta}\sqrt{\frac{\delta}{-x+\delta}} + 2i\lim_{x\to\delta}\sqrt{\frac{\delta}{x-\delta}}\}.$$

In the limit $\delta \to 0$ a Taylor expansion shows that the log-terms vanish whereas the arctan-terms cancel the $i\pi$-contributions such that I remains finite.

In the case $n = 1$ there remains the divergent contribution $\sim \sqrt{\frac{\delta}{x-\delta}}$. Resubstitution of $x = s - (m-1)^2 + \delta$ yields a square-root singularity at $s = (m-1)^2$. As this type of behaviour occurs in the function $W(s_a)$ only which is always multiplied with $s_b - s_c = 2\cos\theta_{ba}\cdot K(s_a)$ we see that the square-root singularity is lifted by the Kacser function K. The case $s = (m-1)^2 + \delta$ leads to the same results in the limit $\delta \to 0$. The resulting amplitudes are thus finite at $s = (m+1)^2 + i\varepsilon$ although discontinuities may occur at this point.

At the unphysical boundary $s = (m+1)^2 - i\varepsilon$ the amplitudes badly diverge as the arctan contribution does not cancel anymore the $i\pi$-terms as above.

Appendix D

Here we give the explicit form of the functions $R^{(I)}$ occuring in the determination of the subtraction polynomial for finite subtraction points, c.f. section 3, eq. (3.29). The derivation employs the identity

$$\begin{aligned}\mathrm{Re}\,\tilde{\Delta}_I(s) &= (s-s_i)(s-s_j)y(s,s_i,s_j)\\ &\quad +\frac{s}{2}\left[s_i\left(y(0,s_i,s_j)+y(0,0,s_i)\right)+(i\leftrightarrow j)\right]\\ &\quad +s_is_jy(0,s_i,s_j),\end{aligned} \tag{D.1}$$

where

$$\tilde{\Delta}_I(s) = \frac{s^2}{\pi}\int_{4m_\pi^2}^{\infty} ds'\frac{\delta^{I,\mathrm{ChPT}}(s')}{s'^2(s'-s-i\epsilon)} \tag{D.2}$$

and

$$y^I(s,s_i,s_j) = \frac{1}{\pi}P\int_{4m_\pi^2}^{\infty} ds'\frac{\delta^{I,\mathrm{ChPT}}(s')}{(s'-s)(s'-s_i)(s'-s_j)}. \tag{D.3}$$

P denotes the principal value and $\delta^{I,\mathrm{ChPT}}$ is the $\pi\pi$-phase with isospin I to leading order in ChPT. For $I = 0, 2$ we thus find

$$\begin{aligned}R^{(I)}(s;s_1,s_2,s_3;s_A) &= \frac{(s_A-s)}{3}\sum_{i<j}^{1,2,3}\Big\{\frac{s}{2}\left[s_i\left(y^I(0,s_i,s_j)+y^I(0,0,s_i)\right)+(i\leftrightarrow j)\right]\\ &\quad -s_is_jy^I(0,s_i,s_j)\Big\}\end{aligned}$$

$$+y^I(s_1,s_2,s_3)\frac{1}{3}\sum_{i<k,k\neq i,j}^{1,2,3}(s-s_i)(s-s_j)(s_A-s_k). \qquad \text{(D.4)}$$

The corresponding expression for $I=1$ is

$$\begin{aligned} R^{(1)}(s_a,s_b,s_c;w_1,w_2) &= \left(\frac{9}{8}s_0^2-\frac{3}{2}s_as_0+\frac{3}{8}s_a^2-\frac{1}{8}(s_b-s_c)^2\right) \\ &\quad\times\left[w_i\left(y^1(0,w_1,w_2)+y(0,0,w_1)\right)+(1\leftrightarrow 2)\right] \\ &\quad+\frac{3}{2}(s_a-s_0)w_1w_2y^1(0,w_1,w_2). \qquad \text{(D.5)} \end{aligned}$$

Tables

SP	s_1	s_2	s_3
-10	-9.6	-9.8	-10.0
-6	-5.6	-5.8	-6.0
-4	-3.5	-3.7	-3.9
-2	-1.7	-1.9	-2.1
0	$5 * 10^{-5}$	$1.2 * 10^{-3}$	$5 * 10^{-3}$
1	1.2	1.33	1.4
2	1.7	1.9	2.1
3	2.6	2.7	2.8

Table 1: Values of the subtraction points SP used in the three times subtracted dispersion relation in units of m_π^2. The subtraction points are the same for U and for V, for W we take the first two values on each row (see also text).

SP	α	β	γ	δ
-10	-1.38	19.73	-7.87	3.74
-6	-1.28	20.52	-5.45	4.00
-4	-1.25	20.97	-3.45	4.13
-2	-1.27	21.39	-1.90	4.22
0	-1.28	21.81	4.09	4.19
1	-1.34	21.99	11.24	3.88
2	-1.38	21.90	17.46	3.44
3	-1.47	21.08	36.67	1.81
error bar	± 0.14	∓ 1.52	± 3.18	∓ 1.08

Table 2: Coefficients of the subtraction polynomial for the sets of subtraction points specified in Table 1. The last line gives the error bar due to the uncertainty in the determination of L_3. All values given here and in the subsequent tables refer to the one-loop value of the constant $\bar{c}$ discussed in section 5.

SP	P	$ReGL$	A_{app}	A_{tot}
-10	0.86	0.64	$1.62 + i0.44$	$1.63 + i0.41$
-6	1.10	0.40	$1.70 + i0.49$	$1.69 + i0.44$
-4	1.21	0.29	$1.69 + i0.50$	$1.67 + i0.44$
-2	1.26	0.24	$1.60 + i0.49$	$1.59 + i0.42$
0	1.40	0.10	$1.57 + i0.50$	$1.57 + i0.41$
1	1.46	0.11	$1.51 + i0.40$	$1.50 + i0.39$
2	1.49	0.01	$1.42 + i0.49$	$1.46 + i0.38$
3	1.58	-0.08	$1.32 + i0.48$	$1.41 + i0.36$

Table 3: The polynomial approximation P and the real part of the dispersive part of the one-loop result, ReGL, in the center of the Dalitz plot. The sum is fixed to give 1.5, the value of the one-loop amplitude. Also the result of the first approximation (including only Φ_{10}) and the total amplitude are given

SP	a	b	c	g	Γ_{+-0}	Γ_{000}	r
-10	-1.27	0.32	0.07	-0.023	$201eV$	$278eV$	1.38
-6	-1.22	0.29	0.08	-0.020	$213eV$	$297eV$	1.40
-4	-1.21	0.30	0.08	-0.017	$211eV$	$295eV$	1.40
-2	-1.21	0.30	0.08	-0.020	$189eV$	$263eV$	1.40
0	-1.16	0.24	0.09	-0.028	$180eV$	$253eV$	1.40
1	-1.04	0.13	0.10	-0.046	$162eV$	$234eV$	1.44
2	-0.97	0.05	0.09	-0.082	$148eV$	$214eV$	1.45
3	-0.78	-0.06	0.08	-0.107	$128eV$	$189eV$	1.48

Table 4: Values of the physical quantities for different subtraction points (three times subtracted dispersion relations).

SP	s_1	s_2
-10	-9.8	-10.0
-6	-5.6	-6.0
-4	-3.7	-3.9
-2	-1.9	-2.1
0	$1.3 * 10^{-3}$	$5 * 10^{-3}$
1	1.2	1.33
2	1.9	2.1
3	2.7	2.8

Table 5: Values of the subtraction points SP in units of m_π^2 for the twice subtracted dispersion relation

SP	a	b	c	Γ_{+-0}	Γ_{000}	r
-10	-0.81	0.12	0.04	$410eV$	$624eV$	1.52
-6	-0.72	0.10	0.06	$277eV$	$423eV$	1.53
-4	-0.77	0.14	0.05	$222eV$	$335eV$	1.51
-2	-0.90	0.20	0.06	$182eV$	$268eV$	1.47
0	-1.14	0.37	0.03	$145eV$	$203eV$	1.40
1	-0.96	0.28	0.04	$120eV$	$173eV$	1.44
2	-0.78	0.20	0.05	$95eV$	$140eV$	1.47
3	-0.71	-0.13	0.02	$78eV$	$117eV$	1.50

Table 6: Values of various physical observables for different subtraction points and two subtractions.

	$\delta\bar{c}/\bar{c} = +25\%$	$\delta\bar{c}/\bar{c} = -25\%$
$\delta\bar{d}/\bar{d} = +25\%$	$0.15 + i0.04$	$-0.13 - i0.03$
$\delta\bar{d}/\bar{d} = -25\%$	$0.18 + i0.05$	$-0.09 - i0.02$

Table 7: Change of the reduced decay amplitude $\bar{A}$ at the center of the physical decay region for a relative error of 25 % on constants $\bar{c}$, $\bar{d}$.

Figure captions

Fig. 1a Integration contour for case i)

Fig. 1b Integration contour for case ii)

Fig. 1c Integration contour for case iii)

Fig. 1d Integration contour for case iv)

Fig. 2 Lattice of points for the numerical determination of the different functions

Fig. 3 Real part of the decay amplitude for $s = u$ (in units of m_π^2) for $SP = 0$. The full line is the numerical solution of the coupled integral equations as described in the text. Also shown is the current algebra prediction (dashed) and the chiral perturbation theory one-loop result (dotted). The physical region lies between the two vertical lines.

Fig. 4 Imaginary part of the decay amplitude for $s = u$ (in units of m_π^2) for $SP = 0$. The full line is the result of the numerical iteration and the dotted one the chiral perturbation theory one-loop approximation.

Figures

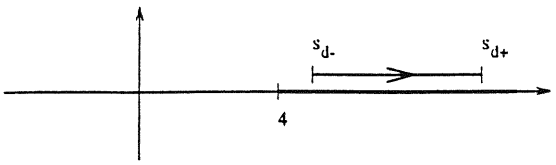

Fig. 1a

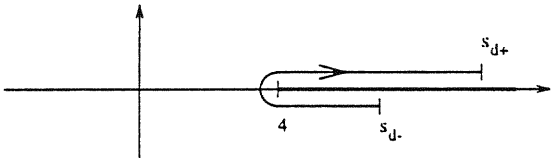

Fig. 1b

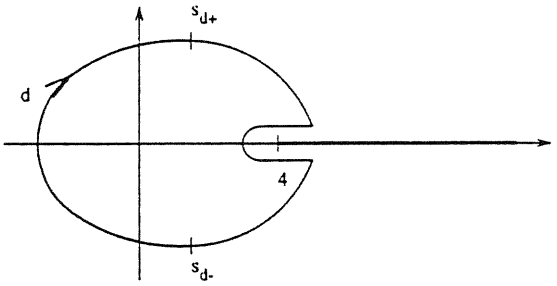

Fig. 1c

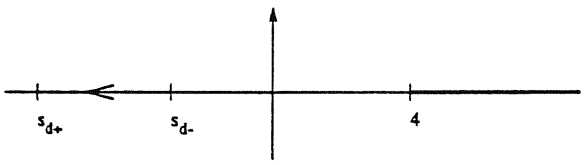

Fig. 1d

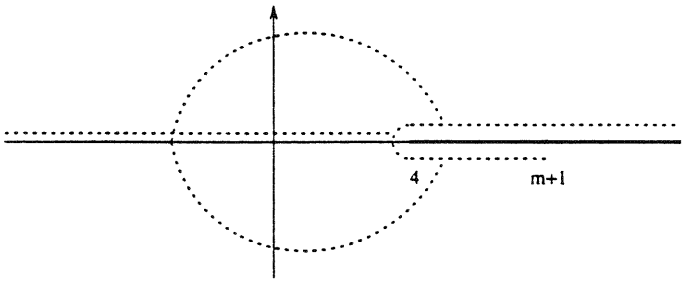

Fig. 2

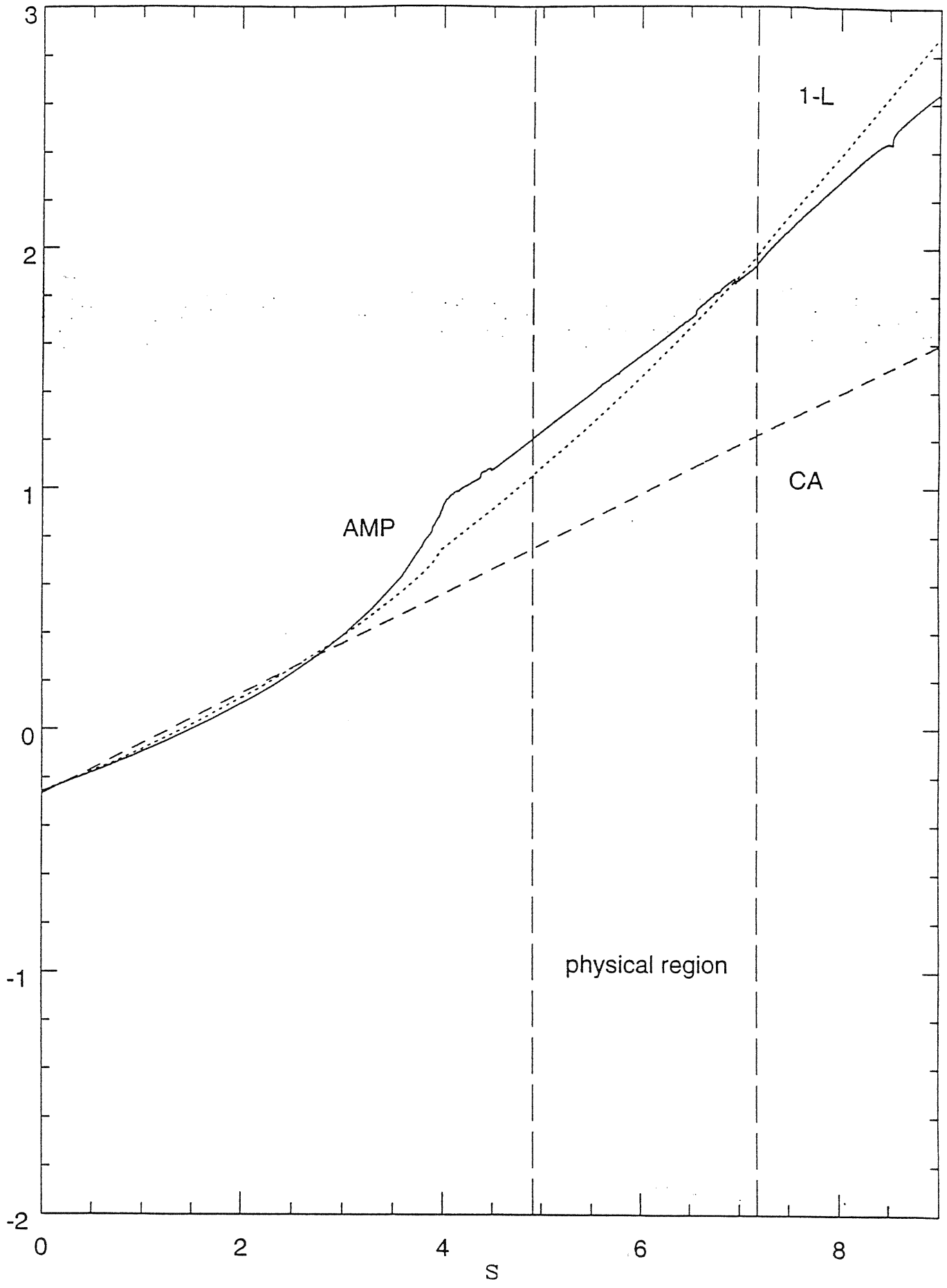

Figure 3

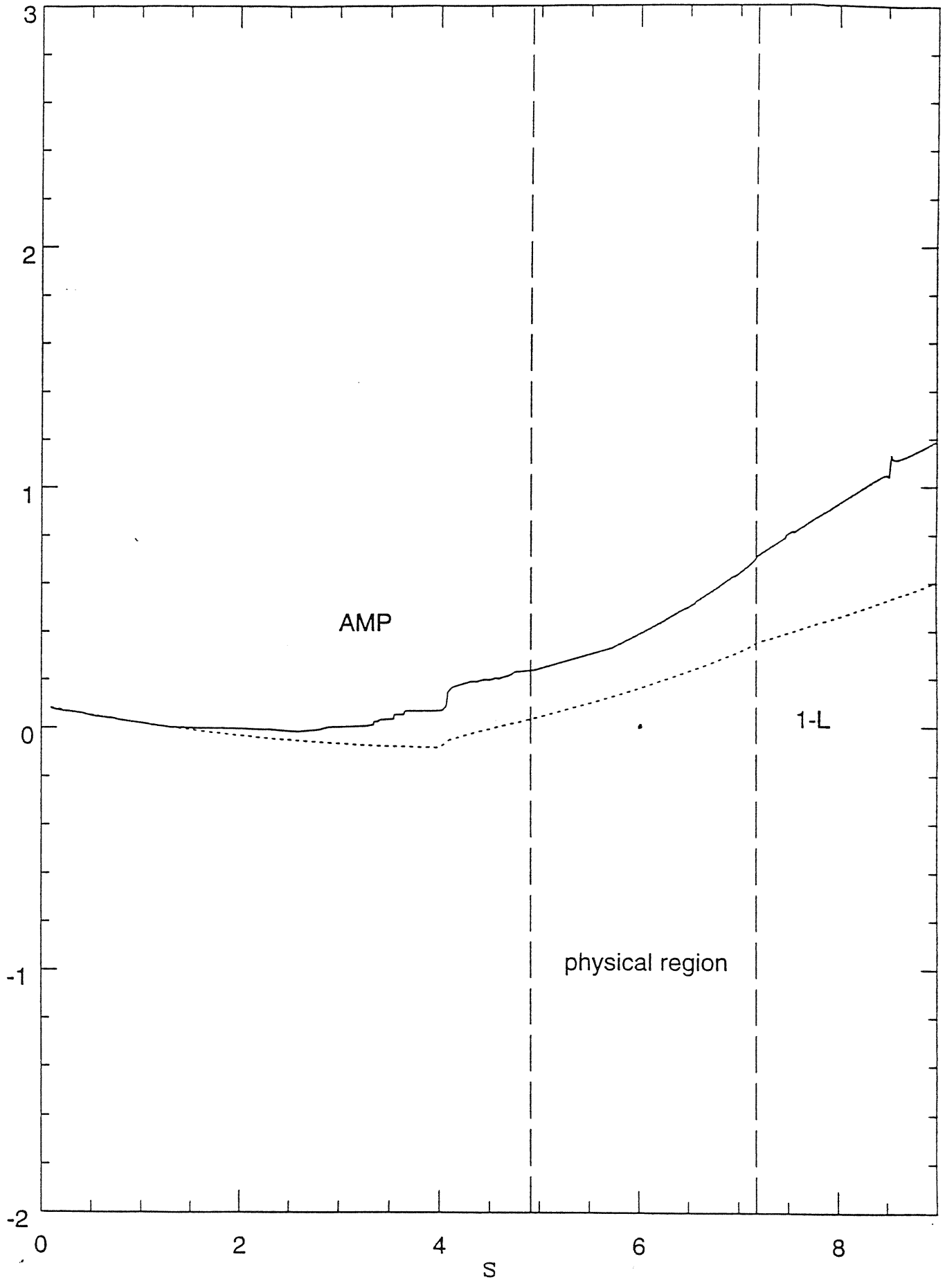

Figure 4